

Alma Mater Studiorum Università di Bologna
Archivio istituzionale della ricerca

New β -Lactam Derivatives Modulate Cell Adhesion and Signaling Mediated by RGD-Binding and Leukocyte Integrins

This is the final peer-reviewed author's accepted manuscript (postprint) of the following publication:

Published Version:

Baiula, M., Galletti, P., Martelli, G., Soldati, R., Belvisi, L., Civera, M., et al. (2016). New β -Lactam Derivatives Modulate Cell Adhesion and Signaling Mediated by RGD-Binding and Leukocyte Integrins. JOURNAL OF MEDICINAL CHEMISTRY, 59(21), 9221-9742 [10.1021/acs.jmedchem.6b00576].

Availability:

This version is available at: <https://hdl.handle.net/11585/585923> since: 2020-02-25

Published:

DOI: <http://doi.org/10.1021/acs.jmedchem.6b00576>

Terms of use:

Some rights reserved. The terms and conditions for the reuse of this version of the manuscript are specified in the publishing policy. For all terms of use and more information see the publisher's website.

This item was downloaded from IRIS Università di Bologna (<https://cris.unibo.it/>).
When citing, please refer to the published version.

(Article begins on next page)

This is the final peer-reviewed accepted manuscript of:

Baiula M, Galletti P, Martelli G, Soldati R, Belvisi L, Civera M, Dattoli SD, Spampinato SM, Giacomini D.

New β -Lactam Derivatives Modulate Cell Adhesion and Signaling Mediated by RGD-Binding and Leukocyte Integrins.

J Med Chem. 2016 Nov 10;59(21):9721-9742. doi: 10.1021/acs.jmedchem.6b00576. Epub 2016 Oct 21. PMID: 27726366.

The final published version is available online at:
<https://pubs.acs.org/doi/10.1021/acs.jmedchem.6b00576>

Rights / License:

The terms and conditions for the reuse of this version of the manuscript are specified in the publishing policy. For all terms of use and more information see the publisher's website.

This item was downloaded from IRIS Università di Bologna (<https://cris.unibo.it/>)

When citing, please refer to the published version.

New β -lactam derivatives modulate cell adhesion and signaling mediated by RGD-binding and leukocyte integrins.

Monica Baiula,^a Paola Galletti,^b Giulia Martelli,^b Roberto Soldati,^b Laura Belvisi,^c Monica Civera,^c Samantha Deianira Dattoli,^a Santi Mario Spampinato^{a}, and Daria Giacomini^{b*}*

^a Department of Pharmacy and Biotechnology, University of Bologna, Via Irnerio, 48, 40126, Bologna, Italy

^b Department of Chemistry "G. Ciamician", University of Bologna, Via Selmi 2, 40126 Bologna, Italy.

^c Department of Chemistry, University of Milan, Via Golgi 19, 20133 Milan, Italy

KEYWORDS. Lactams, integrins, cell adhesion, azetidinones, peptidomimetics, antagonist, agonist.

ABSTRACT. A novel series of β -lactam derivatives that was designed and synthesized to target RGD-binding and leukocyte integrins is reported. The compound library was evaluated by investigating the effects on integrin-mediated cell adhesion and cell signaling in cell lines expressing $\alpha_V\beta_3$, $\alpha_V\beta_5$, $\alpha_V\beta_6$, $\alpha_5\beta_1$, $\alpha_{IIb}\beta_3$, $\alpha_4\beta_1$, and $\alpha_L\beta_2$ integrins. SAR analysis of the new series of azetidinones enabled the recognition of structural elements associated with integrin selectivity. We obtained selective and potent agonists that could induce cell adhesion and promote cell signaling mediated by $\alpha_V\beta_3$, $\alpha_V\beta_5$, $\alpha_5\beta_1$, or $\alpha_4\beta_1$ integrin, and antagonists for the integrins $\alpha_V\beta_3$ and $\alpha_5\beta_1$, as well as $\alpha_4\beta_1$ and $\alpha_L\beta_2$ preventing the effects elicited by the respective endogenous agonists.

INTRODUCTION

β -Lactam compounds represent an important class of four-membered cyclic amides (azetidin-2-ones) thanks to their considerable and diverse biological activities. Azetidinone derivatives first attracted attention for their antibacterial properties, but over the past few decades they have gained importance as inhibitors of various enzymes.¹⁻³ For example, new β -lactam lipopeptides have been reported to inhibit a bacterial signal peptidase,⁴ advances have been reported regarding the use of β -lactams as antagonists of cholesterol absorption,⁵ some azetidinones have been shown to be antagonists of human fatty acid amide hydrolase (hFAAH),⁶ heat shock protein 90,⁷ and histone deacetylases,⁸ and some of their derivatives are antithrombotic agents.⁹

The presence of a β -lactam ring in a series of bioactive molecules with different protein targets allows us to consider that azetidin-2-one is a privileged structure. In particular, β -lactams have two specific structural features that are of interest with regard to biological activity: *i*) a constrained four-membered cyclic amide which could easily undergo ring-opening reactions by nucleophilic residues in the active sites of enzymes; e.g., this mechanism has been suggested to account for antibacterial activity and the inhibition of β -lactamases and elastases; and *ii*) a rigid core structure that, by reducing the conformational degrees of freedom, could favor and actually enhance directional non-covalent bonding for ligand-receptor recognition.¹⁰

Among receptor ligands that are structurally based on the β -lactam core, only a few azetidinones have been shown to exhibit activity against integrins, which are a complex family of cellular receptors (Figure 1).¹¹⁻¹⁴

Integrins are α/β heterodimeric transmembrane proteins that mediate cell-cell and cell-extracellular matrix (ECM) interactions by binding specific ligands. In mammals, 18 α -subunits

and 8 β -subunits assemble into 24 different integrins, which may recognize collagen, laminin, or fibronectin and other ECM proteins. Eight integrins bind to ECM proteins sharing the tripeptide RGD (arginine-glycine-aspartic acid). Conversely, leukocyte integrins involved in immune functions bind proteins containing LDV (leucine-aspartic acid-valine) or related sequences such as LDT (leucine-aspartic acid-threonine) and IDS (isoleucine-aspartic acid-serine) (Figure 2).

RGD integrins can preferentially bind different ECM proteins: $\alpha_v\beta_3$ integrin binds, among others, vitronectin, fibronectin and osteopontin; $\alpha_v\beta_5$ binds vitronectin and fibronectin; $\alpha_{IIb}\beta_3$ recognizes fibrinogen, plasminogen and von Willebrand factor; $\alpha_5\beta_1$ and $\alpha_v\beta_6$ mainly recognize fibronectin.¹⁵ Integrin $\alpha_v\beta_6$ may also bind other RGD-containing peptides such as the latency-associated peptide.¹⁶ The ligand binding specificity seems to be related to the sequences flanking RGD, the auxiliary binding motifs in the ligand, and the conformational presentation of the triad.¹⁷ Numerous $\alpha_v\beta_3$ and $\alpha_5\beta_1$ ligands have been developed; moreover, powerful ligands for specific addressing and blocking of the $\alpha_v\beta_3$ integrin subtype have been published.¹⁸⁻¹⁹ As regards $\alpha_v\beta_5$ and $\alpha_v\beta_6$ integrins, novel ligands have been recently proposed.²⁰⁻²¹

The ability of integrins to bind and associate with various components of the ECM or soluble ligands largely depends on the structural conformations of the two α and β subunits, and distinct conformations are crucial for regulating both inside-out and outside-in cell signaling.^{22,23} Integrins regulate crucial aspects of cellular functions, including migration, adhesion, differentiation, growth and survival, by communicating bidirectional signals between the extracellular and intracellular environments.²⁴

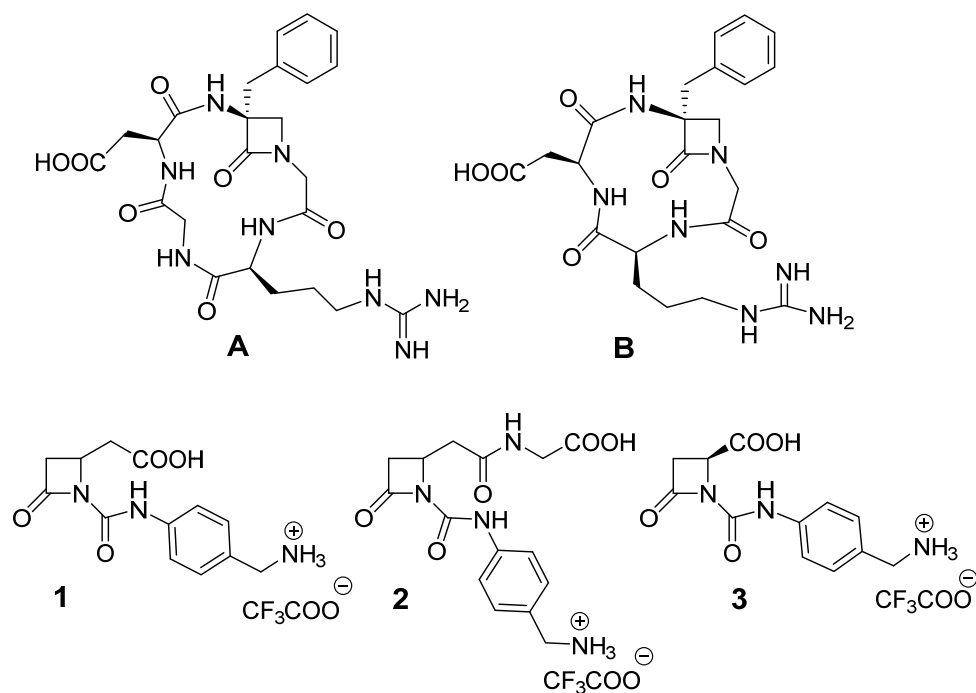


Figure 1. Previously reported β -lactams as integrin ligands.

The crystallization of a soluble integrin heterodimer revealed that integrins exist in an inactive state with their ligand-binding domains facing the cell membrane.²⁵ Activation occurs when membrane-bound proteins increase the affinity of ectodomains for extracellular ligands that promote cell adhesion and modulate intracellular signaling cascades.²⁶ The ligand-binding site forms a region at the intersection of the α and β subunits; as regards RGD integrins, both the α chain²⁷ and β subunit may participate.²⁸

The binding of endogenous ligands to integrins recruits several cellular components and modulates intracellular signaling cascades, especially those leading to the activation of focal adhesion kinase (FAK) and mitogen-activated protein kinase (MAPK) pathways that play a crucial role in the regulation of numerous cell functions.²⁹ The tight regulation of integrin signaling is paramount for normal physiological functions such as migration, proliferation and

differentiation, and misregulated integrin activity is associated with several pathological conditions. Therefore, extensive effort has been made to discover and develop integrin antagonists for use in clinical applications.^{27, 30} To date, most efforts have focused on the development of small molecules or antibodies that can inhibit mainly the following integrins: $\alpha_v\beta_{3/5}$ and $\alpha_5\beta_1$, which have been implicated in tumor development; $\alpha_4\beta_{1/7}$ and $\alpha_L\beta_2$, which have been implicated in the regulation of immune functions, and $\alpha_{IIb}\beta_3$ (GpIIbIIIa), which has been implicated in platelet aggregation.¹⁵ Interestingly, several studies have suggested that small molecules that act as integrin agonists may have therapeutic efficacy. These include an agonist of $\alpha_M\beta_2$ integrin³¹ that ameliorates kidney transplantation,³² an agonist of $\alpha_L\beta_2$ integrin that inhibits lymphocyte trans-endothelial migration,³³ and an agonist of $\alpha_4\beta_1$ integrin that induces progenitor cell adhesion.³⁴ In agreement with these studies, Du *et al.* reported that small RGD peptides that bind to $\alpha_{IIb}\beta_3$ integrin behaved as partial agonists or competitive antagonists of cell adhesion.³⁵ These latter studies suggest that, through modification of the sequence of small peptides or with the use of small molecules, an integrin antagonist could be converted to an agonist that could increase cell adhesion and modulate intracellular signaling pathways.

With regard to β -lactams as integrin ligands, Palomo *et al.* and Aizpurua *et al.* embedded an azetidinone scaffold in cyclic peptides or pseudopeptides that contain the RGD recognition motif or a RGD-like sequence (Figure 1, **A** and **B**).¹¹⁻¹³ The incorporation of conformational constraints, such as the β -lactam scaffold inserted in a cyclic peptide in this case, was, in general, intended to enhance selectivity and modulate the affinity toward the receptor.

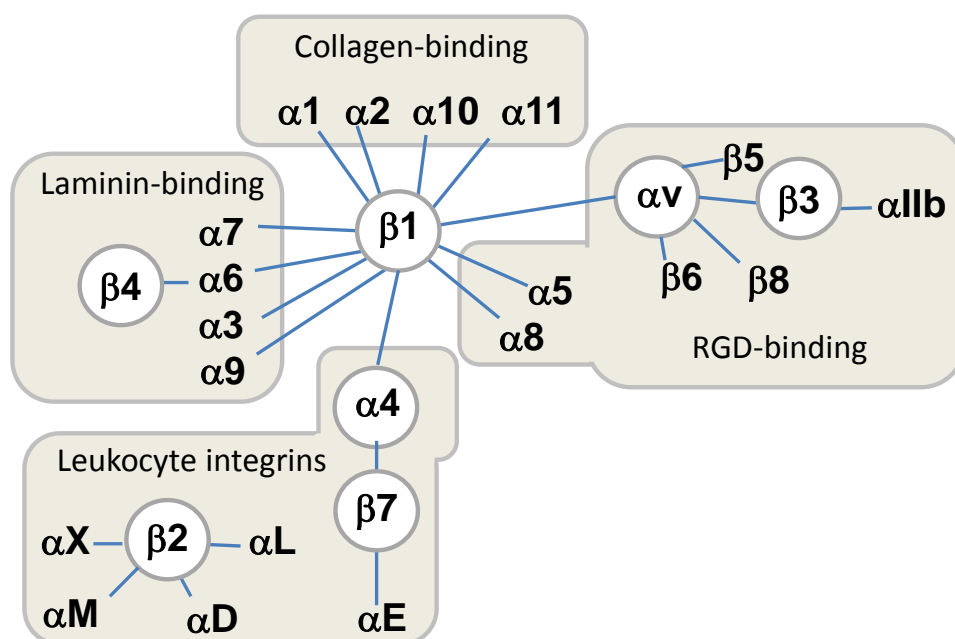


Figure 2. Classification of heterodimeric integrins according to specific combinations of the α and β chains.

Recently, we reported a preliminary study on the design and synthesis of three new azetidiones as potential integrin ligands **1-3** (Figure 1).¹⁴ The approach used for the design of the new molecules was based on rationalization from known integrin ligands. We set out to explore molecules that contained azetidione as a rigid cyclic central core, with two arms holding the carboxylic acid and a basic moiety, as in the RGD sequence, with a spacing of 9 to 14 atoms. The 4-amidobenzylamine residue was chosen as a basic terminus that was directly linked to the β -lactam nitrogen atom as in urea derivatives, and a carboxylic acid was located on the C-4 side chain. When these new molecules were tested on cell lines K562 (human erythroleukemia expressing $\alpha_5\beta_1$ integrin) and SK-MEL-24 (human malignant melanoma expressing $\alpha_v\beta_3$ integrin), we observed the concentration-dependent enhancement of fibronectin-mediated

adhesion. In particular, β -lactam **1** has a higher affinity toward $\alpha_5\beta_1$ integrin (EC_{50} 12 nM) and β -lactam **2** is more selective for integrin $\alpha_v\beta_3$ (EC_{50} 11 nM).¹⁴

Herein we describe the synthesis of a small library of new β -lactam derivatives (Chart 1) that were specifically designed by a structure-based strategy to target particular classes of integrins. The biological activities of these new compounds were evaluated by investigating their effects on integrin-mediated cell adhesion in suitable cell lines expressing the RGD integrins $\alpha_v\beta_3$, $\alpha_v\beta_5$, $\alpha_v\beta_6$, $\alpha_5\beta_1$ and $\alpha_{IIb}\beta_3$, and leukocyte integrins $\alpha_4\beta_1$ and $\alpha_L\beta_2$; furthermore, their effects on cell signaling activated by integrins $\alpha_v\beta_3$, $\alpha_5\beta_1$, $\alpha_{IIb}\beta_3$, $\alpha_4\beta_1$ and $\alpha_L\beta_2$ were investigated. A structure-activity analysis of this new series of azetidinones allowed us to identify structural elements associated with integrin selectivity and, by adopting this approach, we obtained selective and potent agonists that could induce cell adhesion mediated by $\alpha_v\beta_3$, $\alpha_v\beta_5$, $\alpha_5\beta_1$, or $\alpha_4\beta_1$ integrin, and antagonists for $\alpha_v\beta_3$, $\alpha_v\beta_6$ and $\alpha_5\beta_1$, as well as $\alpha_4\beta_1$ and $\alpha_L\beta_2$.

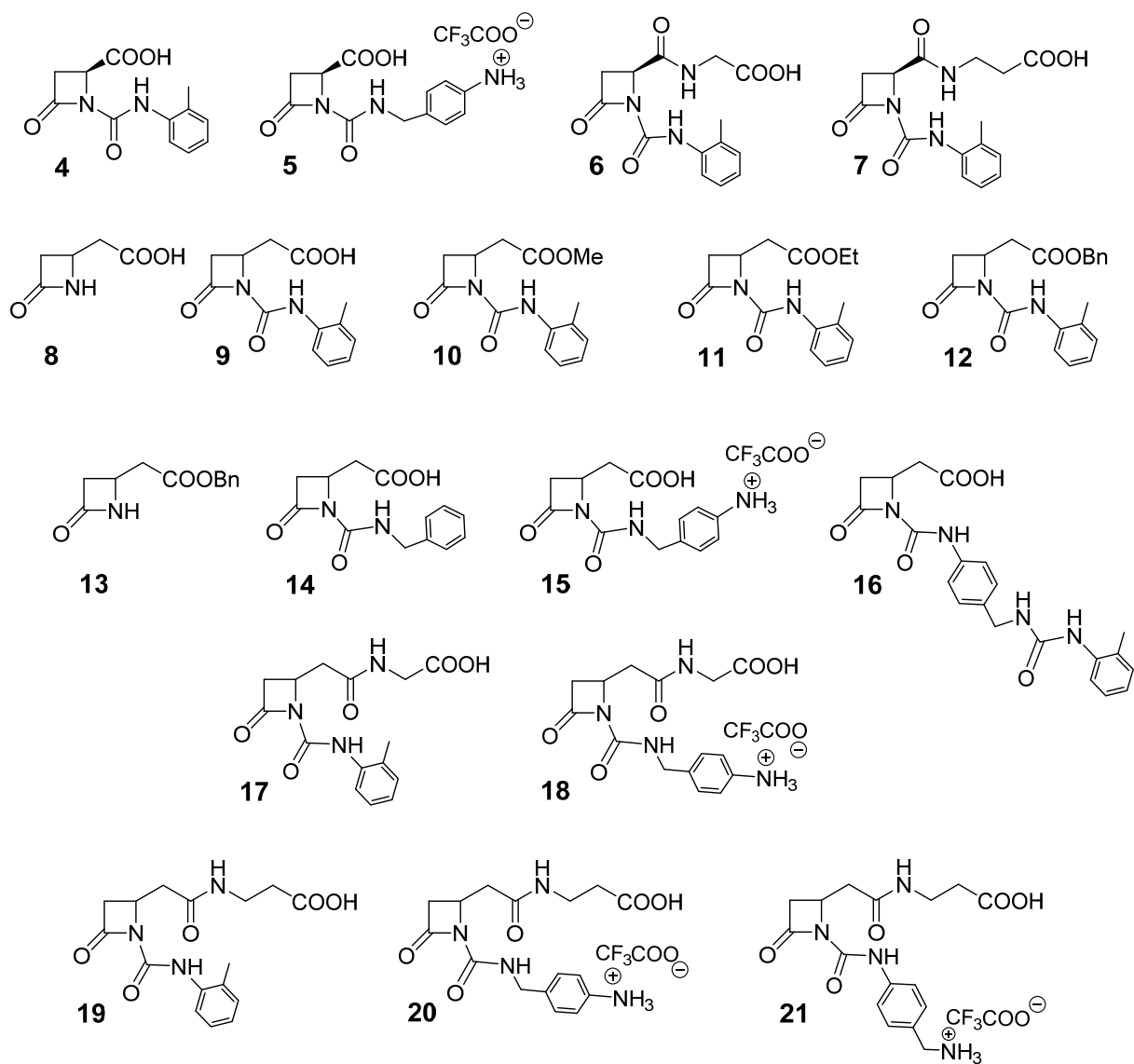


Chart 1. β -Lactam compounds evaluated in this study.

RESULTS AND DISCUSSION

Synthesis.

We were intrigued by the possibility of using only a β -lactam core to obtain a constrained molecule that could favor complexation with the receptor, excluding the insertion of an azetidinone ring in cyclic peptides (Figure 1). The β -lactam ring represents a site of conformational restriction with a cyclic β -amino acid residue³⁶ which could give a favorable alignment of both the amine and carboxylate moieties on the ligand, which would satisfy the crucial requirements for integrin affinity and selectivity.³⁷

Of the various integrin ligands explored by others, we were particularly interested in the antagonists reported by Tolomelli et al.³⁸⁻⁴¹ They found that a 4-aminobenzyl-amide residue was an effective Arg mimetic with an increased affinity for $\alpha_v\beta_3$ and $\alpha_5\beta_1$ integrins, whereas the presence of a 4[[*N*-2-methylphenyl]ureido]-phenylacetyl motif (PUPA) greatly enhanced bioactivity and specificity for $\alpha_4\beta_1$ integrins.⁴²

We chose to install a 4-aminobenzyl-amido- or its isomeric 4-aminomethyl-phenyl-amido-residue on the N-1 nitrogen atom of the azetidinone *via* a condensation reaction with isocyanates (Figure 3). These two isomeric substitutions were selected to evaluate the influence of the basicity of the amine terminus; in this case we compared benzylamine and aniline residues.⁴³

The carboxylic acid function which could coordinate at the metal ion-dependent adhesion site (MIDAS) of the β -subunit of integrins³⁷ was placed on the C-4 side chain of the azetidinone. In detail, β -lactams **4-7** (Chart 1) have a C-4 carboxylic acid residue, as either a free acid or dipeptide, and compounds **8-21** have a C-4 acetic acid residue, as either a free acid, ester or

dipeptide. In dipeptide derivatives, two amino acids were coupled with the azetidinone carboxylic acid, and glycine or β -alanine was chosen to have un-substituted flexible chains. For compounds **1-3**, a panel of 18 new azetidinones was synthesized starting from two commercially available compounds, L-aspartic acid and 4-acetoxy-azetidinone. The general synthetic approach is depicted in Figure 3. Compounds **4-7** were prepared starting from L-aspartic acid, cyclization to give azetidin-2-one 3-carboxyester, insertion of the imide by condensation with an isocyanate, and C-4 side chain elongation *via* a peptide-coupling procedure. The C-4 acetic acid derivatives **8-21** were synthesized from the commercially available 4-acetoxy-azetidinone with a Reformatsky reagent by benzyl bromoacetate.⁴⁴⁻⁴⁶ Again, the imido group was obtained with the appropriate isocyanate and peptide coupling gave higher molecular weight derivatives.

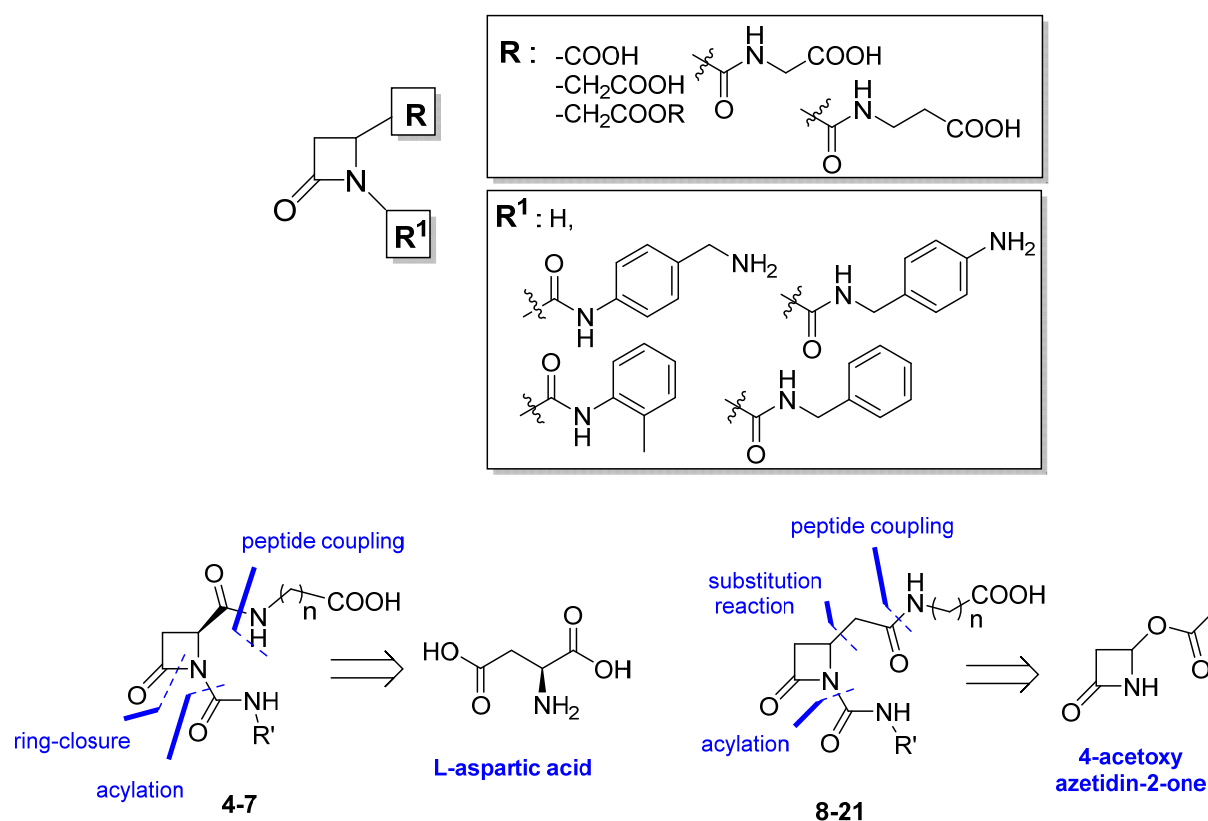
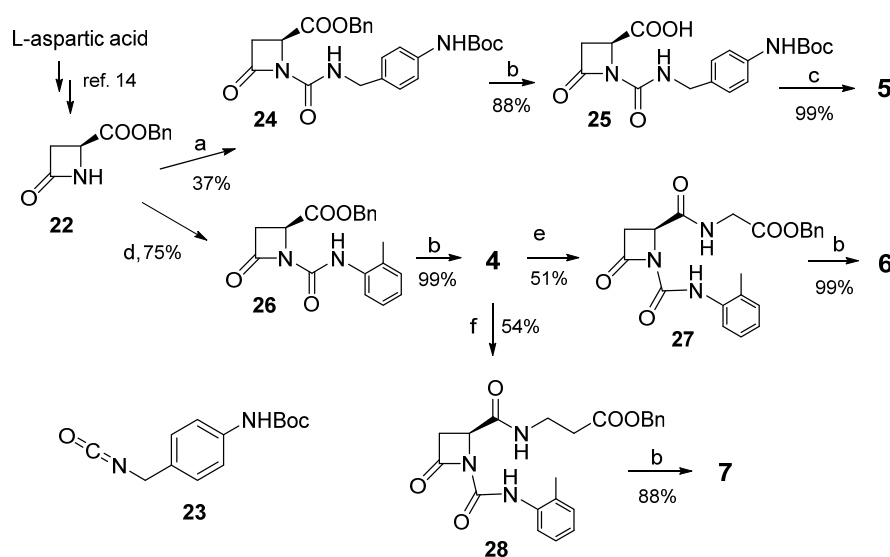


Figure 3. Substituent variations and synthetic strategies for β -lactams **4-21**.

A careful strategy for protecting the carboxylic acid and the amine terminus was developed to preserve the β -lactam ring throughout the synthesis, and in particular in the final deprotection step. Particular attention was paid to specific combinations of temporary or permanent protecting groups to achieve full or partial deprotection depending on the requirements of the synthetic strategy. The synthesis of compounds **4-21** is described in detail in Schemes 1-4.

The 4-carboxylic-azetidin-2-one benzyl ester **22** was obtained in a two-step procedure starting from L-aspartic acid as previously reported¹⁴ (Scheme 1). Treatment of **22** with NaHMDSA in THF at -78°C and *tert*-butyl(4-(isocyanatomethyl)phenyl)carbamate **23**, freshly prepared with triphosgene (see the Experimental Section), gave **24**. Hydrogenolysis gave the corresponding acid **25** and final treatment with trifluoroacetic acid (TFA) furnished compound **5** as a trifluoroacetate salt.

Scheme 1. Synthesis of β -lactams **4-7**^a



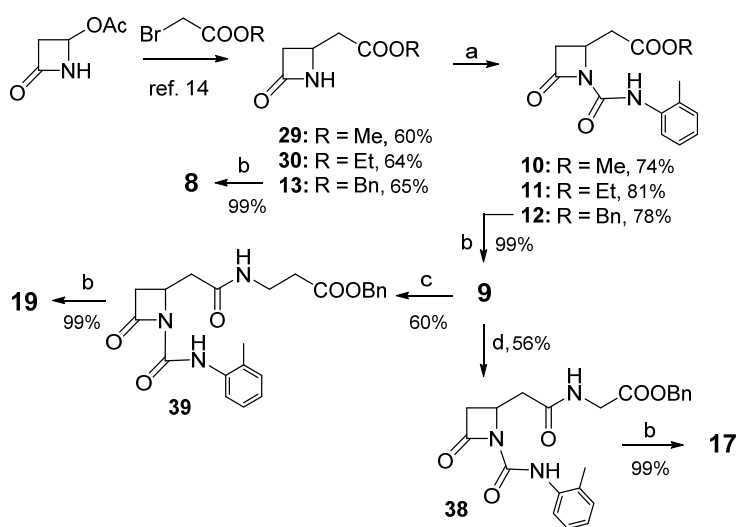
^a Reagents and conditions: (a) NaHMDSA, *tert*-butyl(4-(isocyanatomethyl)phenyl)carbamate **23**, THF, -78°C, 1h; (b) H₂, Pd/C 10%, THF/MeOH = 1:1, rt, 2h; (c) TFA, CH₂Cl₂, 0°C then rt 24 h; (d) K₂CO₃, *o*-tolyl isocyanate, CH₃CN, 2h, rt; (e) oxalylchloride, TEA, CH₂Cl₂, glycine benzylester-HCl, DMAP, rt, 16h; (f) oxalylchloride, TEA, CH₂Cl₂, β-alanine benzylester-PTSA, DMAP, rt, 16h.

Compound **26** was obtained from **22** with the commercially available *o*-tolyl isocyanate in acetonitrile and potassium carbonate. Subsequent hydrogenolysis gave **4** in good yields. The carboxylic acid **4** was coupled with glycine benzylester or β-alanine benzylester to give compounds **27** and **28**, respectively. Finally, azetidinones **6** and **7** were obtained from **27** and **28** by hydrogenolysis.

The syntheses of β-lactams **8-21** include a common origin: a substitution reaction on the 4-acetoxy azetidinone by a Reformatsky reagent as outlined in Scheme 2. Methyl-, ethyl-, or benzyl-bromoacetates were treated with an excess of metallic Zn in THF to furnish the corresponding Reformatsky reagents which were then coupled with 4-acetoxyazetidin-2-one to give 4-acetate-azetidin-2-one esters **29**, **30**, and **13** in good overall yields after flash chromatography¹⁴ (Scheme 2). Treatment of the three esters with *o*-tolyl isocyanate under basic conditions provided the imido-azetidinones **10**, **11**, and **12**. Azetidinones **8** and **9** were then obtained by hydrogenolysis from **13** and **12**, respectively. The azetidinone **9** was subjected to peptide coupling with glycine benzylester or β-alanine benzylester with EDC as a coupling reagent, TEA, and a catalytic amount of dimethylaminopyridine (DMAP) to give the intermediates **38** and **39**, which were deprotected by hydrogenolysis to give **17** and **19**, respectively (Scheme 2). The N-1-side chain was inserted on azetidinone **13**, which had been

previously deprotonated at -78°C with sodium hexamethyl disilylamide (NaHMDSA), with *tert*-butyl(4-(isocyanatomethyl)phenyl) carbamate **23** (Scheme 3), which had been obtained in turn from 4-*N*-Boc-aminobenzylamine with triphosgene (see the Experimental Section for details).

Scheme 2. Synthesis of β -lactams **8-13**, **17**, and **19**^a

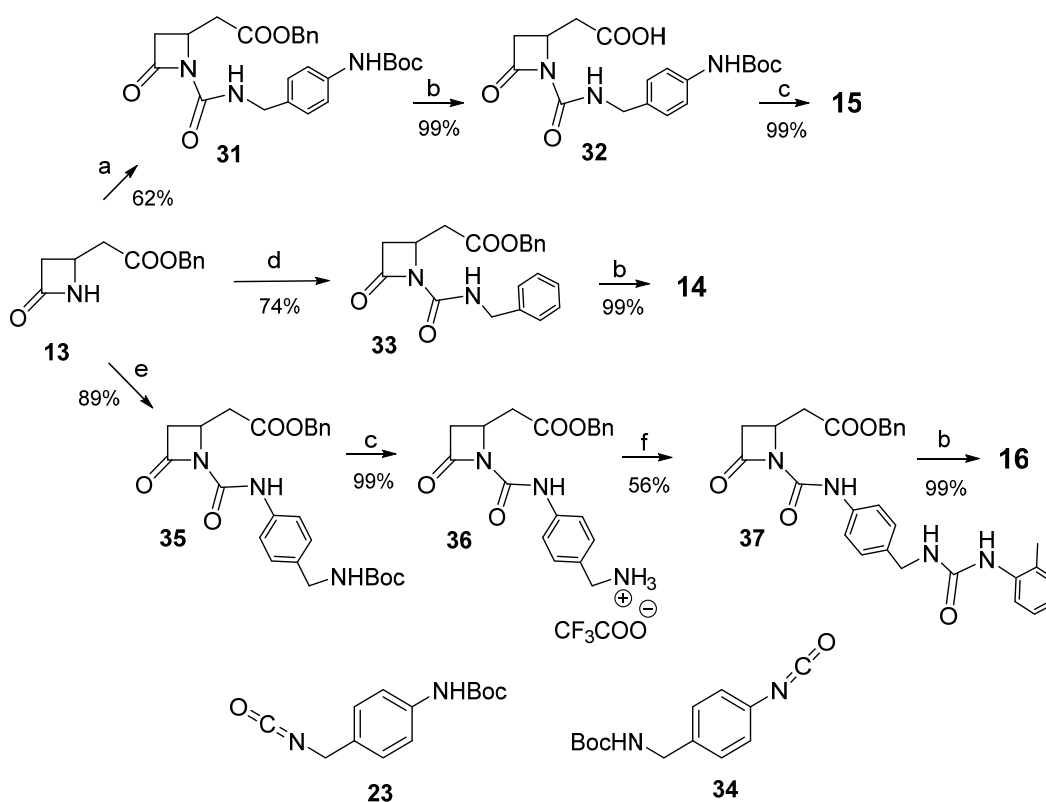


^a Reagents and conditions: (a) K_2CO_3 , *o*-tolyl isocyanate, CH_3CN , 2h, rt; (b) H_2 , THF/MeOH (1:1), Pd/C 10%, 2h, rt; (c) EDC, TEA, DMAP, β -alanine benzylester-PTSA, CH_2Cl_2 , 0°C to rt, 16h; (d) EDC, TEA, DMAP, glycine benzylester-PTSA, CH_2Cl_2 , 0°C to rt. 16h.

Hydrogenolysis of the resulting adduct **31** gave **32**, which in turn provided compound **15** by treatment with trifluoroacetic acid. Azetidinone **36** was obtained by a similar procedure in two steps starting from **13** and *tert*-butyl 4-isocyanatobenzylcarbamate **34** (see the Experimental Section). Treatment of **36** with commercially available *o*-tolyl isocyanate and trimethylamine

gave **37**, which in turn gave azetidinone **16** by hydrogenolysis. Compound **14** was obtained in two steps from **13** by condensation with commercially available benzyl isocyanate and hydrogenolysis. Azetidinones **18** and **20** were obtained from carboxylic acid **32** by peptide coupling with glycine benzyl ester or β -alanine benzyl ester, respectively (Scheme 4).

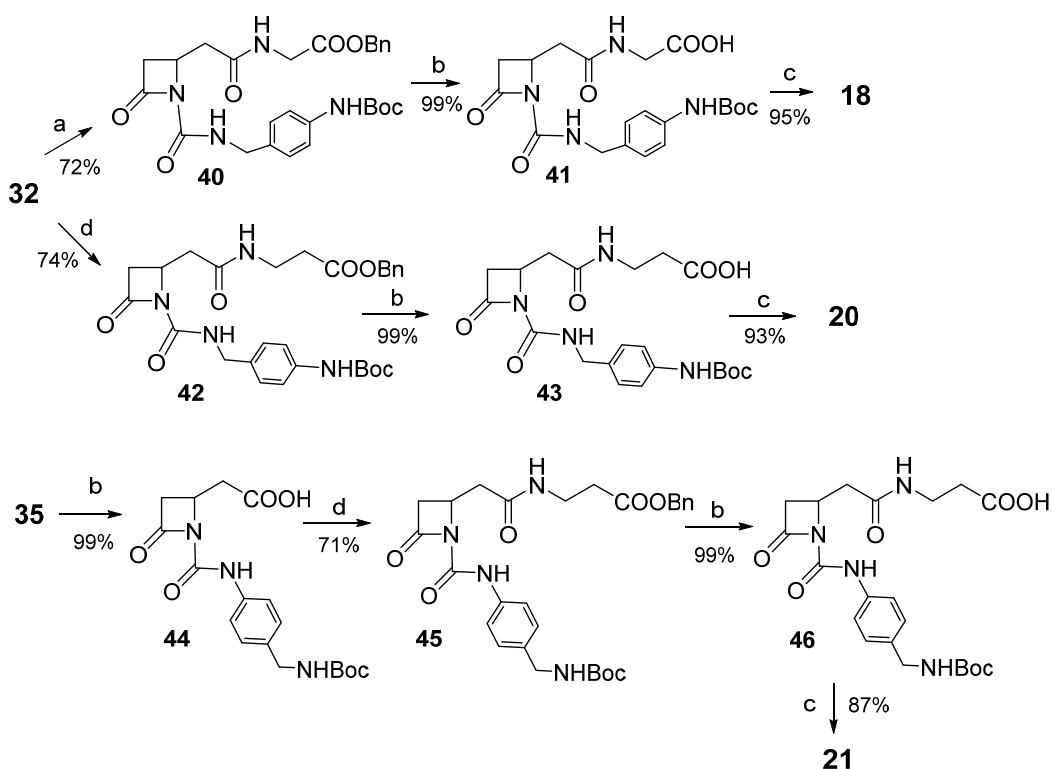
Scheme 3. Synthesis of β -lactams **14-16**^a



^a Reagents and conditions: (a) NaHMDSA, *tert*-butyl(4-(isocyanatomethyl)phenyl)carbamate **23**, THF, -78°C , 1h; (b) H_2 , Pd/C 10%, THF/MeOH = 1:1, rt, 2h; (c) TFA, CH_2Cl_2 , 0°C then rt, 24 h; (d) K_2CO_3 , benzyl isocyanate, CH_3CN , 2h, rt; (e) NaHMDSA, *tert*-butyl 4-isocyanatobenzylcarbamate **34**, THF, -78°C , 1h; (f) TEA, *o*-tolyl isocyanate, 0°C then rt, 2h.

When intermediates **40** and **42** were subjected to a two-step procedure consisting of hydrogenolysis and treatment with TFA for the final deprotection, compounds **18** and **20** were obtained in very good yields. Preliminary hydrogenolysis of compound **35** gave the intermediate **44**, which, via peptide coupling with β -alanine benzylester, hydrogenolysis and treatment with TFA, gave the final compound **21** (Scheme 4).

Scheme 4. Synthesis of β -lactams **18**, **20**, and **21**.^a



^a Reagents and conditions: (a) DCC, TEA, DMAP, CH_2Cl_2 , glycine benzylester-PTSA, 0°C to rt, 16h; (b) H_2 , Pd/C 10%, THF/MeOH = 1:1, rt, 2h; (c) TFA, CH_2Cl_2 , 0°C then rt, 24 h; (d) DCC, TEA, DMAP, β -alanine benzylester-PTSA, CH_2Cl_2 , 0°C to rt, 16h.

Cell adhesion and solid-phase binding assays

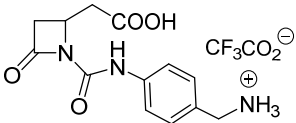
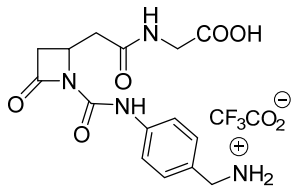
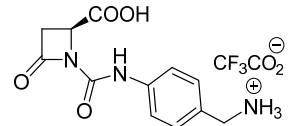
To investigate the activity and selectivity profiles of β -lactam derivatives, we performed adhesion assays with different cell lines expressing the RGD integrins $\alpha_v\beta_3$, $\alpha_v\beta_5$, $\alpha_v\beta_6$, $\alpha_5\beta_1$ and $\alpha_{IIb}\beta_3$ or leukocyte integrins $\alpha_4\beta_1$ and $\alpha_L\beta_2$. In these assays, cells were seeded onto plates coated with specific substrates and allowed to adhere before the number of adherent cells was determined in the presence of increasing concentrations of the test compounds (1×10^{-10} M - 1×10^{-4} M). The peptides H-Gly-Arg-Gly-Asp-Thr-Pro-OH (**47**), Ac-Asp-Arg-Leu-Asp-Ser-OH (**48**),³⁸ cyclo(-Arg-Gly-Asp-D-Phe-Val) (**49**),⁴⁷⁻⁴⁸ (N-[[4-[[[(2-methylphenyl)amino]carbonyl]amino]-phenyl]acetyl]-l-leucyl-l-aspartyl-l-valyl-l-proline (**50**) (BIO-1211)⁴⁹ and Tirofiban (**51**)⁵⁰ were included as reference ligands for the various integrins assayed. Novel ligands that inhibited cell adhesion promoted by fibronectin, fibrinogen, VCAM-1 or ICAM-1 were referred to as antagonists, whereas compounds that increased fibronectin- or fibrinogen- or VCAM-1- or ICAM-1-mediated cell adhesion were considered to be agonists. All of the β -lactam derivatives that were effective in cell-adhesion tests are summarized in Table 1, whereas compounds **6**, **10**, **11**, **12**, **13**, **16**, and **18** were completely inactive and their data are not shown. Integrin selectivity of each compound for one or more integrins over others assayed is also shown in Table 1.

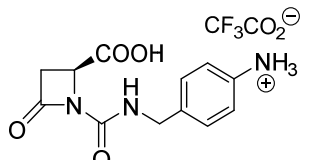
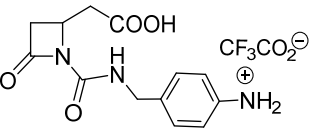
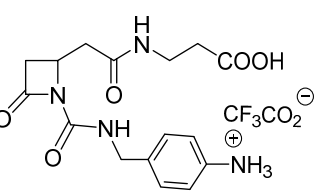
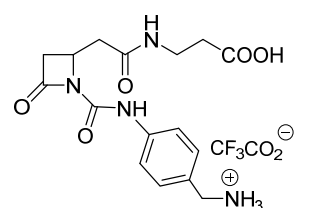
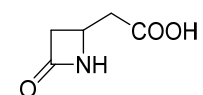
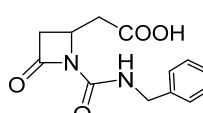
Any potential cell toxicity of β -lactams under investigations was evaluated by Annexin V-7-AAD assay by flow cytometry. We observed that all compounds (10^{-4} M) added for three hours to the cell lines used in this study did not cause any cell necrosis and/or apoptosis (data not shown).

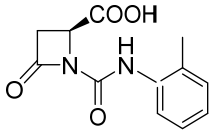
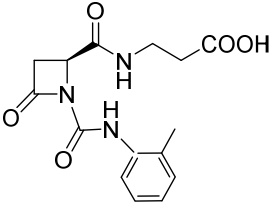
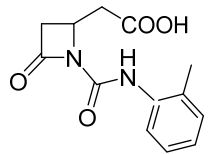
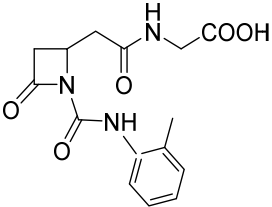
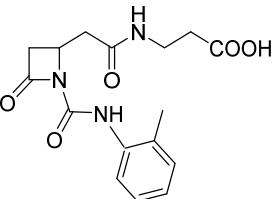
The preliminary results showed an unexpected activity of azetidinones **1** and **2** as promoters of cell adhesion mediated by $\alpha_5\beta_1$ and $\alpha_v\beta_3$ integrins,¹⁴ with an interesting potency at the

nanomolar level (Table 1). Compound **1** was not able to discriminate between $\alpha_v\beta_3$ and $\alpha_5\beta_1$ integrins whereas **2** preferentially activated $\alpha_v\beta_3$ integrin.

Table 1. Effects of active β -lactam compounds on RGD-binding and leukocyte integrin-mediated cell adhesion. Data are presented as EC_{50} for agonists (in bold), and as IC_{50} for antagonists (nM)^a. The ability of β -lactams to increase or inhibit cell adhesion mediated by a specific integrin ligand (fibronectin for $\alpha_5\beta_1$, $\alpha_v\beta_3$ and $\alpha_v\beta_6$, fibrinogen for $\alpha_v\beta_5$ and $\alpha_{IIb}\beta_3$, VCAM-1 for $\alpha_4\beta_1$, and ICAM-1 for $\alpha_L\beta_2$) was evaluated.

comp. number	structure	RGD-binding integrins					Leukocyte integrins		Preferential selectivity ^h
		$\alpha_v\beta_3$	$\alpha_v\beta_5$	$\alpha_v\beta_6$	$\alpha_5\beta_1$	$\alpha_{IIb}\beta_3$	$\alpha_4\beta_1$	$\alpha_L\beta_2$	
1		55.00 ± 0.04^b agonist	5.09 ± 0.07 agonist	167 ± 6 agonist	12.00 ± 0.02^b agonist	> 5000	> 5000	2410 ± 64 antagonist	$\alpha_v\beta_5$ and $\alpha_5\beta_1$
2		11.00 ± 0.03^b agonist	505 ± 17 agonist	> 5000	763.00 ± 0.08^b agonist	> 5000	> 5000	> 5000	$\alpha_v\beta_3$
3		> 5000 ^b	> 5000	> 5000	365.00 ± 0.05^b agonist	> 5000	> 5000	> 5000	$\alpha_5\beta_1$

5		> 5000	> 5000	> 5000	525.0 ± 1.2 antagonist	> 5000	8.8 ± 0.8 antagonist	> 5000	$\alpha_4\beta_1$
15		71.7 ± 0.5 antagonist	> 5000	> 5000	44.5 ± 2.6 agonist	> 5000	574.0 ± 1.7 antagonist	0.39 ± 0.02 antagonist	$\alpha_L\beta_2$ and $\alpha_V\beta_3$
20		> 5000	> 5000	> 5000	1050 ± 17 antagonist	> 5000	> 5000	> 5000	$\alpha_5\beta_1$
21		> 5000	> 5000	> 5000	6.7 ± 0.6 agonist	1563 ± 69	> 5000	> 5000	$\alpha_5\beta_1$
8		40.9 ± 0.8 antagonist	376 ± 15 agonist	> 5000	1031 ± 35 agonist	311 ± 35 agonist	> 5000	1627 ± 23 antagonist	$\alpha_V\beta_3$
14		> 5000	> 5000	> 5000	417 ± 6 antagonist	> 5000	> 5000	> 5000	$\alpha_5\beta_1$

4		352 ± 7 antagonist	> 5000	> 5000	158 ± 4 antagonist	> 5000	1.39 ± 0.04 antagonist	> 5000	α ₄ β ₁
7		active ligand ^c	> 5000	> 5000	> 5000	> 5000	> 5000	> 5000	α _v β ₃
9		> 5000	> 5000	> 5000	> 5000	> 5000	12.9 ± 0.6 agonist	> 5000	α ₄ β ₁
17		> 5000	> 5000	> 5000	9.9 ± 0.1 agonist	> 5000	> 5000	> 5000	α ₅ β ₁
19		187 ± 3 agonist	670 ± 24 agonist	44.4 ± 0.8 antagonist	49.0 ± 2.9 agonist	> 5000	17.4 ± 0.8 antagonist	> 5000	α ₄ β ₁

47	H-Gly-Arg-Gly-Asp-Thr-Pro-OH	925.5 ± 6.3 antagonist	34.2 ± 0.7 antagonist	> 5000	0.62 ± 0.09 antagonist	> 5000	nd ^d	nd
48	Ac-Asp-Arg-Leu-Asp-Ser-OH ^e	25 ± 3 antagonist	2278 ± 0.07 antagonist	> 5000	> 5000	> 5000	nd	nd
50	BIO-1211 ^f	nd	nd	nd	nd	nd	8.6 ± 1.5 antagonist	0.84 ± 0.19 antagonist
49	Cyclo(-Arg-Gly-Asp-D-Phe-Val) ^g	146 ± 43 antagonist	16.0 ± 1.3 antagonist	3696 ± 38 antagonist	nd	nd	nd	nd
51	Tirofiban	nd	nd	nd	nd	9.4 ± 0.8 antagonist	nd	nd

-
- a) Values represent the mean ± SD of three independent experiments carried out in quadruplicate.
- b) Data preliminarily reported in ref. 14
- c) Compound **7** showed a peculiar behavior: at low concentrations (10^{-10} - 10^{-7} M) it behaves as antagonist while it acts as an agonist at higher concentrations (10^{-6} – 10^{-4} M).
- d) nd = not determined
- e) See ref. 38
- f) See ref. 49
- g) See ref. 47 and 48.
- h) Defined as at least a 0.7 log difference in pIC₅₀ values among the assayed integrins; see ref. 51.

The most interesting β -lactam compounds behaving as integrin ligands in the cell adhesion assays above described, were further characterized in solid-phase competitive integrin binding assays set up for $\alpha_v\beta_3$, $\alpha_v\beta_5$, $\alpha_v\beta_6$, $\alpha_5\beta_1$, $\alpha_{IIb}\beta_3$, and $\alpha_L\beta_2$, whereas affinity to $\alpha_4\beta_1$ was evaluated by a scintillation proximity-binding assay (SPA). Interestingly, as reported in Table 2, the assayed compounds showed affinity values and selectivity that agree with the data found in cell adhesion assays reported in Table 1; an exception was **8** that, in comparison to cell adhesion assays, was 20 times more potent *vs.* $\alpha_v\beta_3$ and 370 times more potent *vs.* $\alpha_v\beta_5$ in solid-phase binding assays (Table 2).

Table 2. IC₅₀ values (nM)^a of β -lactam compounds on RGD-binding and leukocyte integrins.

Comp.	RGD-binding integrins					Leukocyte integrin $\alpha_4\beta_1$	Preferential selectivity ^b
	$\alpha_v\beta_3$	$\alpha_v\beta_5$	$\alpha_v\beta_6$	$\alpha_5\beta_1$	$\alpha_{IIb}\beta_3$		
1	5.6 ± 0.9	3.8 ± 1.3	80.5 ± 12.6	5.5 ± 1.1	>1000	>1000	$\alpha_v\beta_3$, $\alpha_v\beta_5$, $\alpha_5\beta_1$
2	1.2 ± 0.3	103.7 ± 23.2	>1000	>1000	>1000	>1000	$\alpha_v\beta_3$
5	>1000	>1000	>1000	331 ± 36	>1000	7.6 ± 1.3	$\alpha_4\beta_1$
15	9.9 ± 2.2	>1000	>1000	9.7 ± 2.4	>1000	498 ± 27	$\alpha_L\beta_2$, ^c $\alpha_v\beta_3$, $\alpha_5\beta_1$
21	>1000	>1000	>1000	5.5 ± 0.8	>1000	nd ^d	$\alpha_5\beta_1$
8	1.9 ± 0.6	2.4 ± 0.8	>1000	>1000	265 ± 69	>1000	$\alpha_v\beta_3$, $\alpha_v\beta_5$
4	285 ± 17	>1000	>1000	114 ± 9	nd	1.1 ± 0.1	$\alpha_4\beta_1$
9	>1000	>1000	>1000	>1000	nd	9.8 ± 0.8	$\alpha_4\beta_1$
17	>1000	>1000	>1000	52.0 ± 2.6	nd	>1000	$\alpha_5\beta_1$
19	116 ± 9	634 ± 28	23.4 ± 5.3	36.0 ± 5.7	nd	12.4 ± 1.1	$\alpha_4\beta_1$, $\alpha_v\beta_6$, $\alpha_5\beta_1$
49	1.4 ± 0.4	14.2 ± 6.3	>1000	nd	>1000	nd	

51 nd nd nd nd 7.3 ± 0.7 nd

- a) IC₅₀ for RGD-binding integrins and $\alpha_L\beta_2$ was determined by a competitive solid-phase binding assay to specific ligand (fibronectin for $\alpha_v\beta_3$, $\alpha_v\beta_6$, and $\alpha_5\beta_1$, fibrinogen for $\alpha_v\beta_5$ and $\alpha_{IIb}\beta_3$, and ICAM-1 for $\alpha_L\beta_2$). IC₅₀ for $\alpha_4\beta_1$ was determined by scintillation-proximity assay (SPA). Values represent the mean ± SD of three independent experiments carried out in duplicate.
- b) Defined as at least a 0.7 log difference in pIC₅₀ values among the assayed integrins; see ref. 51.
- c) Compound **15** was the unique that retained a relevant $\alpha_L\beta_2$ binding affinity (IC₅₀ 6.7 ± 2.5, n=3).
- d) nd = not determined

With regard to $\alpha_v\beta_3$ integrin, no structural variation improved fibronectin-mediated cell adhesion, and **1** and **2** were confirmed to be the most active agonists of this series vs $\alpha_v\beta_3$. Among the new derivatives, azetidinones **15** and **8**, which have either a less basic aniline terminus (**15**) or a carboxylic acid terminus alone (**8**), reduced cell adhesion mediated by $\alpha_v\beta_3$ integrin, and thus displayed antagonist activity. Compound **7** with an acidic terminus of β -alanine and an ureido PUPA motif behaves as an antagonist towards $\alpha_v\beta_3$ integrin at low concentrations, and as an agonist at higher concentrations. Aizpurua and colleagues have described low molecular weight β -lactam pseudopeptides which fulfilled several structural requirements to act as antagonists or agonists at $\alpha_v\beta_3$ integrin by differently regulating genes known to be related to angiogenesis in an in vitro cell assay.¹¹ Interestingly, a shorter acidic side chain, as in **4**, acts as a low potent antagonist, whereas a longer one, as in **19**, switched the activity to agonism.

As regards solid-phase binding assays, **1**, **2**, **15**, and **8** exhibited a nanomolar activity towards $\alpha_v\beta_3$ integrin (Table 2). Azetidinone **1** possessed a remarkable affinity towards $\alpha_v\beta_5$, $\alpha_v\beta_6$, and $\alpha_5\beta_1$ integrin. Compound **2** exhibited an 8.5 times higher activity for $\alpha_v\beta_3$ integrin in comparison to $\alpha_v\beta_5$ and did not recognize the other integrins evaluated in the solid-phase binding assays.

Azetidinone **8** binds to $\alpha_v\beta_3$ and $\alpha_v\beta_5$ integrin in a nanomolar range; **19** exhibited a 96 times lower potency compared to **2** towards $\alpha_v\beta_3$ integrin.

Compounds **1** and **8** acted as agonists in cell adhesion assays towards $\alpha_v\beta_5$ integrin (Table 1) and retained a relevant affinity for this integrin in solid-phase binding assays (Table 2); **1** exhibited a similar affinity towards $\alpha_5\beta_1$ integrin and **2** and **19** were far less active.

With regards to $\alpha_v\beta_6$ integrin, **1** and **19** were the most effective in cell adhesion assays: **1** behaved as an agonist whereas **19** was an antagonist (Table 1). This latter compound was the most potent towards $\alpha_v\beta_6$ integrin albeit it binds to $\alpha_5\beta_1$ and $\alpha_4\beta_1$ integrin with similar activities. Solid-phase binding assays confirmed the affinity of **1** and **19** to $\alpha_v\beta_5$ integrin; both compounds also bind to $\alpha_v\beta_3$, $\alpha_v\beta_5$ and $\alpha_5\beta_1$ integrin (Table 2).

With regard to $\alpha_5\beta_1$ integrin, compounds **1**, **21**, and **17** appeared to be the most potent agonists at promoting cell adhesion, with EC_{50} values of 12.0, 6.7 and 9.9 nM, respectively (table 1). Moreover, **21** and **17** were relatively selective agonists for $\alpha_5\beta_1$ over the other integrins assayed. The inhibition of $\alpha_5\beta_1$ -mediated cell adhesion was observed only at a micromolar range for a few derivatives with a short carboxylic acid terminus on C-4, and a less basic or PUPA residue on the nitrogen (**5**, **14**, and **4**, Table 1). Interestingly, **3** and **5**, despite a low potency for the $\alpha_5\beta_1$ receptor, showed opposite activities, in that **3** was an agonist whereas **5** was an antagonist of cell adhesion. A similar result was observed for **20** and **21**: the former, with an aniline residue, was a weak antagonist ($IC_{50} > 1000$ nM) whereas the latter, with a benzylamine terminus, was a strong agonist ($EC_{50} = 6.7$ nM)(Table 1).

A more basic amine terminus (benzylamine versus aniline residues) tended to favor agonist behavior (see, for instance, **1**, **2**, and **3** vs. **5**, **15**, and **20**, Table 1), although these β -lactams could

act as electrostatic clamps for $\alpha_5\beta_1$ or $\alpha_v\beta_3$ integrins, like the RGD peptide (see modeling section). On the other hand, the presence of an acidic terminus alone with a suitable chain length could allow a favorable interaction at the MIDAS, which could affect cell adhesion. In fact, esters **10**, **11**, **12**, and **13**, which lack these characteristics, were completely inactive toward all the integrins, as were compounds **16** and **18** with longer side chains (table 1).

Compounds **1** and **15** displayed a potent binding affinity towards $\alpha_5\beta_1$ integrin and bind with a similar potency to $\alpha_v\beta_3$ (Table 2). Furthermore, **21** and **19** displayed high affinity for $\alpha_5\beta_1$ integrin; however, **21** was inactive towards the other integrins assayed whereas **19** recognized almost of all of them (Table 2).

Apart **8**, all the selected β lactam compounds were inactive for integrin $\alpha_{IIb}\beta_3$. Azetidinone **8** showed a low affinity either in the cell adhesion assay (EC_{50} 311 nM, Table 1)), acting as an agonist, and in solid-phase binding assay (IC_{50} 265 nM, Table 2)).

We extended our investigation to leukocyte integrins $\alpha_4\beta_1$ and $\alpha_L\beta_2$. Compounds **5** and **4** with a short carboxylic acid terminus or either a less basic or no amine residue efficiently interacted with $\alpha_4\beta_1$ integrin by inhibiting VCAM-1-mediated cell adhesion with IC_{50} values of 8.8 and 1.39 nM, respectively (Table 1). When the amine terminus was replaced with a PUPA residue, we observed increased activities for **4**, **9**, and **19** at a nanomolar level. Conversely, compound **9**, which is a homolog of **4** at the C4, was an effective and very selective agonist of cell adhesion mediated by $\alpha_4\beta_1$ integrin (EC_{50} = 12.9 nM, Table 1), and this activity decreased with an increase in the length of the side chain (**9** vs **17**, Table 1).

In this series of new β -lactam derivatives, we did not find a correlation between the activities toward $\alpha_4\beta_1$ and $\alpha_5\beta_1$ integrins: most of the β -lactams that were active toward the former integrin

were inactive toward the latter. Compound **19** is an exception in this sense, because it showed similar potencies for opposite activities: agonist toward $\alpha_5\beta_1$ ($EC_{50} = 49$ nM), but antagonist toward $\alpha_4\beta_1$ ($IC_{50} = 17.4$ nM) (Table 1).

Adopting a scintillation proximity-binding assay (SPA), we confirmed that **5**, **4**, **9** and **19** bind to $\alpha_4\beta_1$ integrin in a nanomolar range, and that **9** was the most selective recognizing only $\alpha_4\beta_1$ (Table 2).

With regard to β -lactam activity toward $\alpha_L\beta_2$ integrin, only **15** showed excellent activity as an antagonist at subnanomolar concentrations ($IC_{50} = 0.39$ nM, Table 1), albeit it was not selective relative to the other integrins assayed. Furthermore, **15** was the only β -lactam that binds to $\alpha_L\beta_2$ ($IC_{50} 6.7 \pm 2.5$, $n=3$) in solid-phase binding assays.

The abilities of the new β -lactams acting as integrin agonists to increase cell adhesion were tested in the absence of fibronectin for $\alpha_5\beta_1$ and $\alpha_v\beta_3$ or VCAM-1 for $\alpha_4\beta_1$ integrin. For this purpose, the adhesion of K562, SK-MEL-24 and Jurkat E6.1 cells was evaluated in wells that had been previously coated by passive adsorption with each novel agonist under investigation (2-10 $\mu\text{g/mL}$). Regarding $\alpha_5\beta_1$ integrin, β -lactam agonists **15**, **17**, **19**, and **21** induced a significant concentration-dependent increase in K562 cell adhesion, as observed for fibronectin (see the Supporting Information, Figure S1 A); we previously demonstrated the same behavior for β -lactam $\alpha_5\beta_1$ agonists **1** and **2**¹⁴. Pre-incubation of K562 cells with c(-RGDfV) (1 μM), a well known antagonist of RGD integrins,⁴⁷ significantly reduced cell adhesion mediated by azetidiones **15** and **19** but not by **17** and **21** (Supporting Information, Figure S1 A). These results could suggest that β -lactams **15** and **19** may bind the MIDAS site, an effect prevented by c(-RGDfV). Conversely, **17** and **21** might bind to an allosteric site since cell adhesion mediated

by these compounds was preserved even in the presence of c(-RGDfV). Future studies will better address this hypothesis.

As regards $\alpha_v\beta_3$ integrin, SK-MEL-24 cell adhesion was increased in a concentration related-manner by **1** and **2** as well as by fibronectin (see the Supporting Information, Figure S1 B). Pre-incubation with c(-RGDfV) (1 μ M) significantly reduced cell adhesion mediated by **1** and **2**, thus suggesting that both molecules may bind to the MIDAS site.

In addition, compound **9** the only $\alpha_4\beta_1$ agonist, significantly augmented Jurkat E6.1 cell adhesion, similarly to VCAM-1 (Supporting Information, Figure S1 C). Pre-incubation with a neutralizing antibody against the α_5 , α_v , or α_4 integrin subunits (10 μ g/mL) blocked the augmented adhesion of K562 or SK-MEL-24 or Jurkat E6.1 cells induced by β -lactam agonists **1**, **2**, **15**, **17**, **19**, and **21**, respectively (Supporting Information, Figure S1). These results are consistent with the notion that cell adhesion mediated by the new β -lactam agonists effectively and specifically involves $\alpha_5\beta_1$, $\alpha_v\beta_3$ and $\alpha_4\beta_1$ integrins, respectively.

We and others have previously demonstrated that the protein kinase C (PKC) activator PMA (phorbol myristate acetate), which induces megakaryocytic differentiation of the human erythroleukemia cell line K562 (which mainly expresses $\alpha_5\beta_1$ integrin), increases $\alpha_{IIb}\beta_3$ integrin expression,^{14, 52} and this may represent an additional target of these novel β -lactams. To elucidate the contribution of $\alpha_{IIb}\beta_3$ integrin to cell adhesion induced by agonists **15**, **17**, **19**, and **21**, the selective $\alpha_{IIb}\beta_3$ antagonist Tirofiban (**51**) (5 and 10 μ M) was used. Interestingly, **51** did not modify cell adhesion induced by **15**, **17** or **19** (Supporting Information, Figure S1 D), which, at least in this cell line, seems to be mediated only by $\alpha_5\beta_1$ and not by $\alpha_{IIb}\beta_3$ integrin. On the contrary, **51** partially blocked K562 adhesion mediated by compound **21**, meaning that both $\alpha_5\beta_1$

and $\alpha_{11b}\beta_3$ integrins may contribute to cell adhesion induced by this β -lactam (Supporting Information, Figure S1 D).

Effects of selected β -lactams on integrin-mediated ERK phosphorylation.

Intracellular signaling generated by the interaction of components of the extracellular matrix (ECM) with selected integrins involves second messengers,⁵³ including extracellular signal-regulated kinases 1 and 2 (ERK1/2).

Since this pathway is impaired in SK-MEL-24 cells,⁵⁴ to investigate the effects of the compounds that had the greatest effects on $\alpha_v\beta_3$ -mediated signaling activation (**2** and **15**), we used HEK293 cells that had been transfected with plasmids expressing the coding sequences of α_v and β_3 integrin (HEK293+ $\alpha_v\beta_3$). β -Lactam agonist **2** significantly increased ERK1/2 phosphorylation in a concentration-dependent manner in HEK293+ $\alpha_v\beta_3$ (Figure 4 A). Moreover, azetidinone **15**, which behaved as an antagonist towards $\alpha_v\beta_3$ integrin, strongly prevented ERK1/2 activation induced by fibronectin (Figure 4 B).

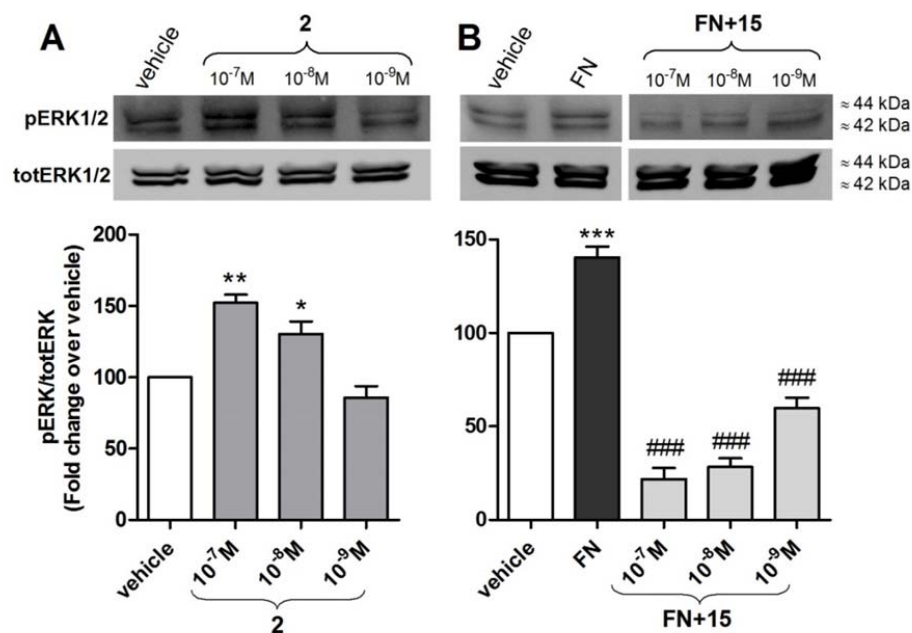


Figure 4. Effects of selected β -lactams on ERK1/2 phosphorylation mediated by $\alpha_v\beta_3$ integrin expressed in HEK293+ $\alpha_v\beta_3$ cells. A. Compound **2** significantly increased, in a concentration dependent manner, ERK1/2 phosphorylation. B. Compound **15** prevented FN-induced phosphorylation of ERK1/2 in a concentration-dependent manner. Representative Western blots show that control cells plated on FN had a much stronger signal for pERK1/2 than vehicle-treated cells (vehicle). Densitometric analysis of the bands is shown (mean \pm SEM; n = 6); the amount of pERK1/2 is normalized to that of totERK1/2. * p < 0.05, **p < 0.01, ***p < 0.001 versus vehicle; ###p < 0.001 versus FN (Newman-Keuls test after ANOVA).

The effects of β -lactams that most strongly affected $\alpha_5\beta_1$ integrin-mediated cell adhesion were evaluated on ERK1/2 phosphorylation in K562 cells. Selected azetidinones that behaved as agonists in the cell adhesion assay, i.e., **15**, **17**, **19**, and **21**, significantly increased ERK1/2

phosphorylation when added alone to cells; moreover, **17**, **19**, and **21** increased ERK1/2 phosphorylation in a concentration-dependent manner (Figure 5 A and B). Otherwise, the $\alpha_5\beta_1$ integrin antagonist **4** reduced ERK1/2 phosphorylation induced by fibronectin in a concentration-related manner (Figure 5 C).

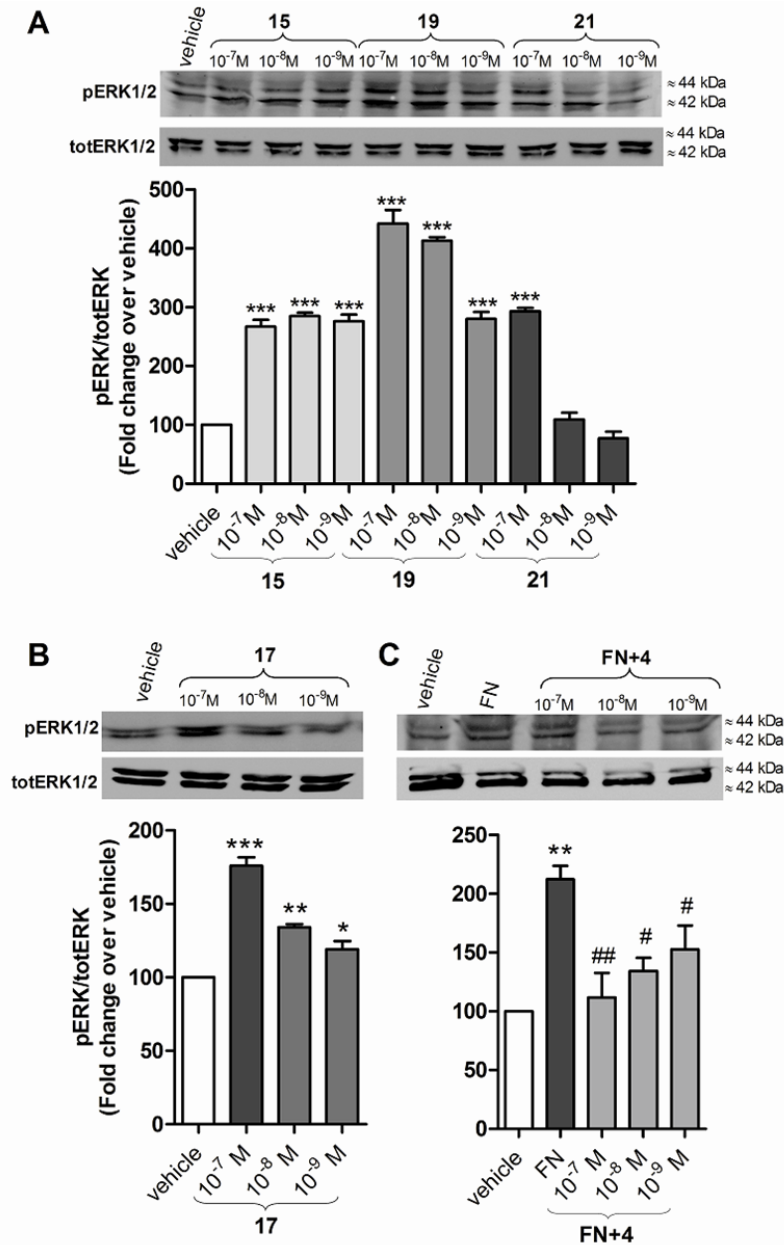


Figure 5. Effects of selected β -lactams on ERK1/2 phosphorylation mediated by $\alpha_5\beta_1$ integrin expressed in K562 cells. A, B: agonists **15**, **17**, **19** and **21** significantly increased ERK1/2 phosphorylation. C: Compound **4** prevented FN-induced phosphorylation of ERK1/2 in a concentration-dependent manner. Representative Western blots show that control cells plated on FN had a much stronger signal for pERK1/2 than vehicle-treated cells (vehicle). Densitometric analysis of the bands is shown (mean \pm SEM; n = 6); the amount of pERK1/2 is normalized to that of totERK1/2. * p < 0.05, ** p < 0.01, ***p < 0.001 versus vehicle; #p < 0.05, ## p < 0.01 versus FN (Newman-Keuls test after ANOVA).

The β -lactam **9**, a selective $\alpha_4\beta_1$ integrin agonist, when added alone to Jurkat E6.1 cells, strongly and significantly increased ERK1/2 phosphorylation in comparison to vehicle-treated cells (Figure 6 A). In Jurkat E6.1 cells exposed to VCAM-1, a significant increase in ERK1/2 phosphorylation was detected (Figure 6 B and C), and pre-incubation with β -lactam antagonists **4**, **5**, and **19** caused a significant decrease in VCAM-1-mediated ERK1/2 phosphorylation (Figure 6 B and C); azetidinones **5** and **19** were effective in a concentration-dependent manner (Figure 6).

Azetidinone **4** was more effective in preventing VCAM-1-induced ERK1/2 phosphorylation at 10^{-9} - 10^{-7} M (Figure 6); lower concentrations (10^{-12} - 10^{-10} M) displayed a concentration-dependent inhibition of ERK1/2 activation by VCAM-1 (Supporting Information, Figure S2).

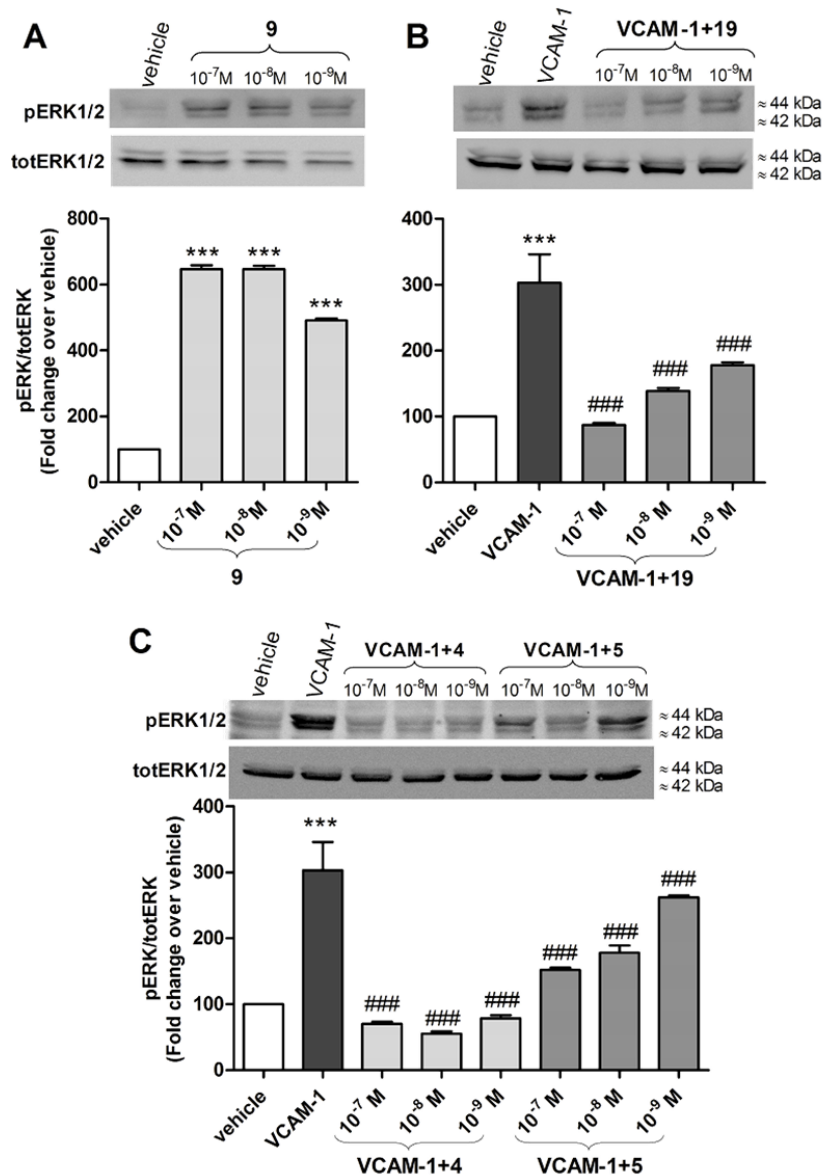


Figure 6. Effects of selected β -lactams on ERK1/2 phosphorylation mediated by $\alpha_4\beta_1$ integrin expressed in Jurkat E6.1 cells. A: β -lactam agonist **9** significantly increased ERK1/2 phosphorylation. B, C: azetidinones **4**, **5**, and **19** prevented VCAM-1-induced phosphorylation of ERK1/2 in a concentration-dependent manner. Representative Western blots show that control cells plated on VCAM-1 had a much stronger signal for pERK1/2 than vehicle-treated cells (vehicle). Densitometric analysis of the bands is shown (mean \pm SEM; n = 6); the amount of

pERK1/2 is normalized to that of totERK1/2.***p < 0.001 versus vehicle; ###p < 0.001 versus VCAM-1 (Newman-Keuls test after ANOVA).

ICAM-1-exposure induced a significant increase in ERK1/2 phosphorylation in Jurkat E6.1 cells by activating $\alpha_L\beta_2$ integrin,⁴⁹ and azetidinone **15**, a $\alpha_L\beta_2$ antagonist, significantly prevented ICAM-1-induced ERK1/2 activation in a concentration-dependent manner (Figure 7).

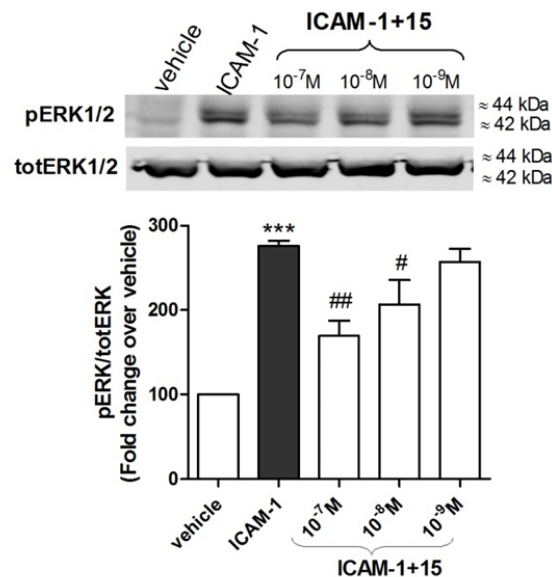


Figure 7. Effects of a selected β -lactam on ERK1/2 phosphorylation mediated by $\alpha_L\beta_2$ integrin expressed in Jurkat E6.1 cells. $\alpha_L\beta_2$ antagonist **15** significantly prevented ICAM-1-induced phosphorylation of ERK1/2 in a concentration-dependent manner. Representative Western blots show that control cells plated on ICAM-1 had a much stronger signal for pERK1/2 than vehicle-treated cells (vehicle). Densitometric analysis of the bands is shown (mean \pm SEM; n = 4); the amount of pERK1/2 is normalized to that of totERK1/2.***p < 0.001 versus vehicle; #p<0.05, ##p < 0.01 versus ICAM-1 (Newman-Keuls test after ANOVA).

β -Lactam binding to $\alpha_4\beta_1$ integrin modulates HUTS-21 epitope exposure in Jurkat E6.1 cells.

Integrins exist in three major conformations: an inactive or bent conformation, an intermediate-activity conformation and a high-activity open conformation.^{55,56} Conformational changes in integrin subunits can be monitored using conformation-specific antibodies that recognize a specific epitope that is exposed only in a defined structural conformation.⁵⁷

To determine whether the binding of these new β -lactams to $\alpha_4\beta_1$ integrin alters its conformation, we used the HUTS-21(PE) monoclonal antibody (mAb), comprising the fluorophore reporter phycoerythrin (PE), that recognizes a LIBS (ligand-induced binding site) epitope that is masked on inactive integrin but is exposed upon agonist binding or partial integrin activation. The epitope recognized by HUTS-21 has been mapped to the hybrid domain of β_1 integrin.⁵⁸ This mAb was added to the cells as described under material and methods, and cells were then analyzed by flow cytometry. As expected, the binding of VCAM-1, the $\alpha_4\beta_1$ endogenous ligand, induced a conformational rearrangement in the β_1 subunit that resulted in exposure of the HUTS-21 epitope and increased antibody binding (Figure 8). Similarly, agonist **9** significantly increased HUTS-21 antibody binding in a concentration-dependent manner. The $\alpha_4\beta_1$ antagonists **4** and **5** significantly and in a concentration-related manner reduced the exposure of HUTS-21 epitope measured as mAb binding (Figure 8).

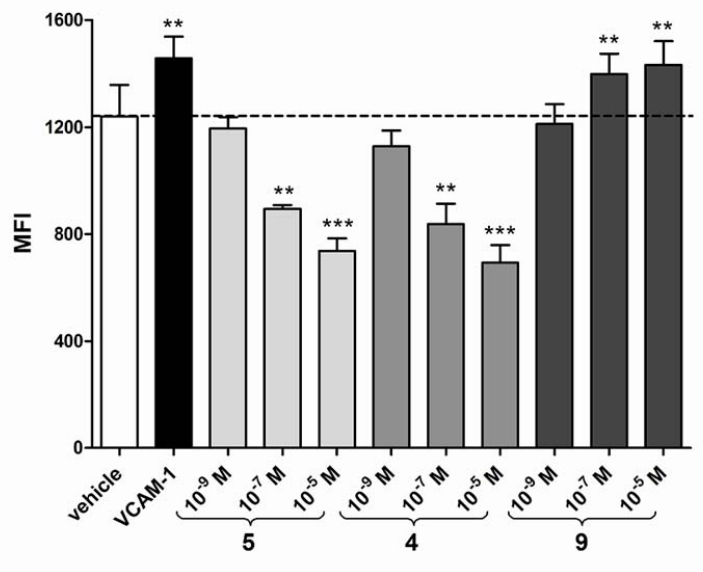


Figure 8. Binding of HUTS-21 antibody to Jurkat E6.1 cells in the presence of different concentrations of the new β -lactams. Jurkat E6.1 cells were incubated with the compounds that had the greatest effects on $\alpha_4\beta_1$ integrin (**4**, **5** and **9**), and HUTS-21 mAb was then added. Flow cytometry analysis of Jurkat E6.1 cells was performed to measure the effects of selected β -lactam agonists and antagonists on exposure of the HUTS-21 epitope. Antagonists **4** and **5** significantly reduced exposure of the HUTS-21 epitope, while β -lactam agonist **9** increased the binding of HUTS-21 mAb to Jurkat E6.1 cells in a concentration-dependent manner. Results are expressed as mean fluorescence intensity (MFI) \pm S. E. M. from four independent experiments carried out in duplicate. MFI values for respective isotype control mAb were set to 0. ** $p < 0.01$, *** $p < 0.001$ versus vehicle (Newman-Keuls test after ANOVA).

Taken together, these data suggest that novel β -lactams acting as $\alpha_4\beta_1$ agonists may induce changes in the integrin conformation, leading to its activation, while $\alpha_4\beta_1$ antagonists may promote inactive or intermediate-activity conformations.

Molecular Modeling

The binding mode of representative β -lactam derivatives to the $\alpha_v\beta_3$ integrin was investigated by a docking approach that was previously developed and successfully applied to the study of small libraries of cyclic and linear RGD peptidomimetics.^{39,59,60} The Glide⁶¹ program V4.5 was used for docking calculations (see the Experimental Section for computational details) and the crystal structure of the extracellular segment of integrin $\alpha_v\beta_3$ in a complex with the cyclic pentapeptide Cilengitide (PDB code 1L5G)⁶² was used as a reference model for interpretation of the results.

The Glide docking protocol was applied to β -lactam derivatives **1** and **15**, which contain the benzylamine and aniline basic moiety, respectively, and the same C-4 acetic acid residue to generate computational models of interaction with the ligand-binding site of the $\alpha_v\beta_3$ integrin. Although we cannot discuss the specific role of a more basic amine terminus (benzylamine versus aniline residues) in favoring agonist behavior on the basis of rigid-protein docking calculations, we can examine the effect of the basic moiety on the ability of the ligand to form an electrostatic clamp and reproduce the crystallographic binding mode of Cilengitide. The enantiomerically pure compound **5**, bearing a C-4 carboxylic acid and an aniline group, was included in the investigation to gain insight into the effect of the distance between the pharmacophoric groups.

Docking runs starting from both enantiomers of compound **1** produced poses that conserved the key polar interactions observed in the X-ray complex. In the calculated poses, the ligand carboxylate group is coordinated to the metal cation in the metal ion-dependent adhesion site (MIDAS) region of the β_3 subunit, and the ligand benzylamine moiety forms salt bridge/H-bond

interactions with the negatively charged side chain of Asp218 in the α_v subunit, although there is no fit with the Arg guanidinium group of Cilengitide (Figure 9). Further stabilizing interactions occur in docking poses of compound **1**, involving the formation of hydrogen bonds between the ligand carboxylate group and the backbone amide hydrogen of Asn215 and Tyr122 in the β unit, and between the ligand β -lactam carbonyl and the β_3 -Arg214 side chain. Ring-stacking or a T-shaped interaction between the ligand aromatic group and the α_v -Tyr178 side chain is also observed in the binding modes calculated for compound **1**.

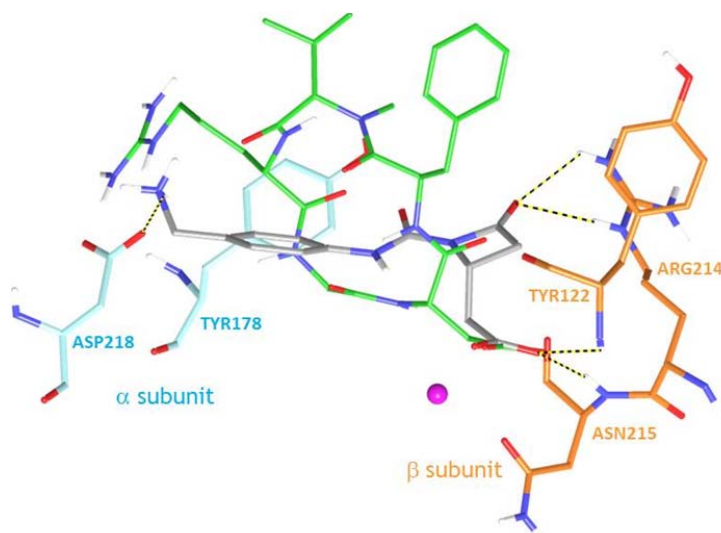


Figure 9. Docking pose of compound (*R*)-**1** (grey carbon atoms) in the crystal structure of the extracellular domain of $\alpha_v\beta_3$ integrin (α unit cyan, β unit orange) overlaid on the bound conformation of Cilengitide (green carbon atoms). Only selected integrin residues involved in interactions with the ligand are shown. The metal ion at MIDAS is shown as a magenta CPK sphere. Non-polar hydrogens are hidden for clarity, while intermolecular hydrogen bonds are shown as dashed lines (H-bond H-O distance between the ligand basic moiety and the α_v -Asp218 carboxylate = 1.9 Å).

Docking runs starting from the two enantiomers of compound **15** produced rather different results. In the calculated poses of (*R*)-**15**, the acid and basic pharmacophoric groups act like an electrostatic clamp and interact with charged regions of the receptor binding site. Nevertheless, a poor fit with the receptor-bound structure of Cilengitide is observed, mainly for the aniline basic moiety (Figure 10), which forms a distorted H-bond with the negatively charged carboxylate of α_v -Asp218. Similar to the observations for compound **1**, one carboxylate oxygen of (*R*)-**15** is coordinated to the MIDAS metal cation, while the second carboxylate oxygen forms H-bonds with the backbone amides of Asn215 and Tyr122 in the β unit. Further stabilizing interactions observed in the binding modes of (*R*)-**15** involve a H-bond between the ligand β -lactam carbonyl and the β_3 -Arg214 side chain, and ring-stacking between the ligand aromatic group and the α_v -Tyr178 side chain.

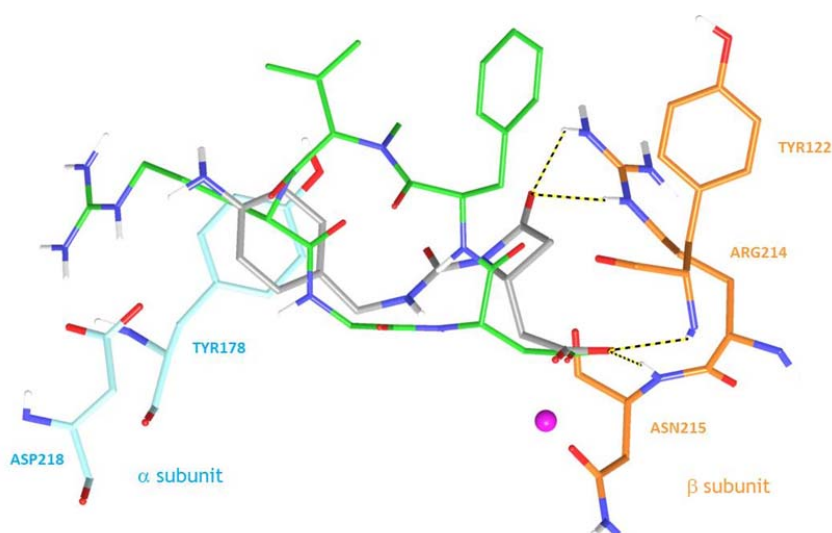


Figure 10. Docking pose of compound (*R*)-**15** (grey carbon atoms) in the crystal structure of the extracellular domain of $\alpha_v\beta_3$ integrin (α unit cyan, β unit orange) overlaid on the bound

conformation of Cilengitide (green carbon atoms). Only selected integrin residues involved in interactions with the ligand are shown. The metal ion at MIDAS is shown as a magenta CPK sphere. Non-polar hydrogens are hidden for clarity and intermolecular hydrogen bonds are shown as dashed lines (H-bond H-O distance between the ligand basic moiety and the α -Asp218 carboxylate = 3.1 Å).

In the calculated poses of (*S*)-**15**, the electrostatic clamp is often lost and the ligand engages in interactions only with the β -subunit. In particular, the coordination of the ligand carboxylate to the MIDAS cation is retained, while the aniline moiety moves toward the β -chain, driven by hydrophobic interactions.

The docking results for compound **5** reveal poor binding ability, in terms of both ligand-receptor interactions and docking score. The shorter distance between the pharmacophoric acid and basic groups (about 11 Å in the docking poses of isomers (*R*)-**1** and (*R*)-**15** shown in Figures 9 and 10 vs. about 9 Å in the poses of compound **5** makes this ligand the worst mimic of the Cilengitide binding mode.

CONCLUSION

We developed a small library of β -lactam derivatives that were specifically designed by a structure-based strategy to target RGD-binding and leukocyte integrins. We obtained selective and potent agonists that could promote cell adhesion mediated by $\alpha_v\beta_3$, $\alpha_v\beta_5$, $\alpha_5\beta_1$, or $\alpha_4\beta_1$ integrin and antagonists that were selective for these RGD-binding integrins as well as antagonists that

bound to $\alpha_v\beta_6$, $\alpha_4\beta_1$ and $\alpha_L\beta_2$ integrins. A benzylamine terminus appeared to favor agonist behavior and this supports the hypothesis that these new β -lactams could act as an electrostatic clamp for $\alpha_5\beta_1$ or $\alpha_v\beta_3$ integrins, as suggested by molecular docking studies at $\alpha_v\beta_3$ receptors. Further investigation of selected β -lactam compounds showed that they could influence intracellular signaling activated by endogenous integrin agonists. Only a few studies have focused on the discovery of integrin agonists that may be useful in several clinical conditions.³¹⁻
³⁴ Interestingly, one of the first studies on RGD mimetic peptides found that they may act as partial agonists as well as competitive antagonists of integrin $\alpha_{IIb}\beta_3$ and proposed that the structural characteristics for peptide activation and the inhibition of endogenous ligand binding are analogous.³⁵ Recently, Van Agthoven *et al.* have described a 10 kDa wild type fibronectin (wtFN10) that binds and activates $\alpha_v\beta_3$ integrin whereas a high-affinity mutant (hFN10), carrying substitutions adjacent to the RGD sequence, behaves as a pure antagonist as it favors an inactive conformation of the integrin. Following selective integrin mutations, hFN10 is switched to a partial agonist.⁶³ Similar conclusions may apply to the present β -lactams, which bind with good affinity to their target integrins and induce a change in conformation that may facilitate cell signaling in the case of agonists or prevent the binding of endogenous ligands in the case of antagonists.

Experimental section

General information

Commercial reagents were used as received without additional purification. ^1H , ^{19}F and ^{13}C NMR spectra were recorded with an INOVA 400 or a GEMINI 200 instrument with a 5 mm probe. All chemical shifts are quoted relative to deuterated solvent signals (δ in ppm and J in Hz). Polarimetric Analyses were conducted on Unipol L 1000 “Schmidt-Haensch” Polarimeter at 598 nm. FTIR spectra: Bruker Alpha instrument, measured as films between NaCl plates, wave numbers are reported in cm^{-1} . The purities of the target compounds were assessed as being >95% using HPLC-MS. HPLC-MS: Agilent Technologies HP1100 instrument, equipped with a ZOBAX-Eclipse XDB-C8 Agilent Technologies column; mobile phase: $\text{H}_2\text{O}/\text{CH}_3\text{CN}$, 0.4 mL/min, gradient from 30 to 80% of CH_3CN in 8 min, 80% of CH_3CN until 25 min, coupled with an Agilent Technologies MSD1100 single-quadrupole mass spectrometer, full scan mode from $m/z = 50$ to 2600, in positive or negative ion mode. Elemental analysis were performed on a Thermo Flash 2000 CHNS/O Analyzer.

β -Lactams **13**, **22**, **35** and **44** were synthesized according to a previously reported procedure.¹⁴ LC-MS and NMR monitoring indicated no degradation for all new β -lactam molecules stored as pure compounds at 4 °C for up to 4 months. As models, we studied the stabilities of compounds **2** and **4** in buffered water solutions at pH = 7.4 at 30 °C and in serum at 30 °C (see Supporting Information).

Isocyanate **23** was synthesized accordingly to a reported procedure,¹⁴ starting from *tert*-butyl (4-(aminomethyl)phenyl)carbamate, which in turns was prepared as in ref. 64. Isocyanate **34** was synthesized according to a previously reported procedure.¹⁴

General procedure for *N*-acylation of β -lactams (GP1A and GP1B)

GP1A: A solution of sodium bis(trimethylsilyl)amide (NaHMDSA) (1.0 M in THF, 1.1 equiv) was added dropwise to a solution of the starting β -lactam **22** or **13** (1 equiv) in anhydrous THF (9 mL/mmol) at -78°C under a nitrogen atmosphere. The mixture was stirred for 15 min, then a solution of freshly prepared isocyanate **23** or **34** (1.5 equiv) in anhydrous THF (1 mL) was added dropwise. After completion (TLC monitoring, 30 min) the mixture was quenched with a saturated solution of NH₄Cl and extracted with AcOEt (10 mL) and with CH₂Cl₂ (2x10 mL). The combined organic extracts were dried over Na₂SO₄, concentrated in vacuum and purified by flash-chromatography affording the desired derivatives **24** or **31**.

GP1B: The starting beta-lactam **22**, **29**, **30** or **13** (1 equiv) was dissolved in anhydrous CH₃CN (1 mL) under a nitrogen atmosphere. Anhydrous and finely ground K₂CO₃ (1.5 equiv) was added, followed by a dropwise addition of the commercially available *o*-tolyl- or benzyl isocyanate (1.2 equiv). The mixture was stirred at room temperature until a complete consumption of the starting beta-lactam (about 2 h, TLC monitoring) and then quenched with a saturated solution of NH₄Cl. The solvent was reduced under vacuum and the residual aqueous solution was extracted with CH₂Cl₂ (3x10mL) The organic layers were collected, dried over Na₂SO₄, concentrated in vacuum and purified by flash-chromatography affording the desired *N*-acylated beta-lactam **26**, **10**, **11**, **12**, or **33**).

General procedure for hydrogenolysis (GP2)

A β -lactam benzyl ester (1 equiv) (**24**, **26**, **27**, **28**, **13**, **12**, **31**, **33**, **37**, **38**, **39**, **40**, **42** or **45**) was dissolved in a mixture of THF and CH₃OH (22 mL/mmol, 1:1 v/v) and Pd on C (10% w/w) was added. The solution was then stirred under a H₂ atmosphere (1 atm) at room temperature. After a complete consumption of the starting material (TLC monitoring, 2 h) the reaction mixture was filtered through celite and concentrated in vacuum. The crude was then triturated with few drops of pentane to afford the desired carboxylic acid (**25**, **4**, **6**, **7**, **8**, **9**, **32**, **14**, **16**, **17**, **19**, **41**, **43** or **46**).

General procedure for N-Boc-deprotection (GP3)

A *N*-Boc-protected β -lactam (1 equiv) (**25**, **32**, **35**, **41**, **43** or **46**) was dissolved in CH₂Cl₂ (18.5 mL/mmol) under a nitrogen atmosphere and trifluoroacetic acid (TFA) (4 equiv) was added dropwise at 0°C. If necessary, a new TFA aliquot (4 equiv) was added after 30 min until a complete conversion, HPLC monitoring). The solvent was removed under reduced pressure and the crude was triturated with few drops of pentane the resulting deprotected compound was thus obtained (**5**, **15**, **36**, **18**, **20** or **21**).

(S)-4-oxo-(*o*-tolylcarbamoyl)azetidine-2-carboxylic acid (**4**)

Following GP2 compound **26** (115 mg, 0.34 mmol) yielded compound **4** as a white solid (83 mg, 99%). IR (film, cm⁻¹) 3339, 1787, 1755, 1737; Mp 121 – 124°C; $[\alpha]_D^{20} = -15$ (c = 1.00, CH₂Cl₂); ¹H NMR (400 MHz, CD₃OD) δ (ppm) 2.30 (s, 3H), 3.13 (dd, *J* = 2.8, 15.8 Hz, 1H), 3.52 (dd, *J* = 6.4, 15.8 Hz, 1H), 4.52 – 4.56 (m, 1H) (d, *J* = 3.6 Hz, 1H), 7.05 – 7.08 (m, 1H), 7.17 – 7.24 (m,

2H), 7.76 (d, $J = 8.0$ Hz, 1H); ^{13}C NMR (100 MHz, CDCl_3) δ (ppm) 17.5, 41.2, 49.3, 121.5, 125.0, 126.7, 128.1, 130.4, 134.5, 147.7, 165.5, 171.8; ESI-MS m/z 247 $[\text{M-H}]^-$. Found C, 57.97; H, 5.02; N, 11.21%; $\text{C}_{12}\text{H}_{12}\text{N}_2\text{O}_4$ requires C, 58.06; H, 4.87; N, 11.29 %.

***(S)*-4-(2-carboxy-4-oxoazetidine-1-carboxamidomethyl) benzenaminium 2,2,2-trifluoroacetate**
(5)

Following GP3, compound **25** (35 mg, 0.96 mmol) was treated with TFA (137 μL , 1.82 mmol, 19 equiv) yielding compound **5** (36 mg, 99%) as a waxy solid. IR (film, cm^{-1}) 3362, 1780, 1698, 1677; $[\alpha]_{\text{D}}^{20} = -3$ ($c = 0.86$, CH_3OH); ^1H NMR (400 MHz, CD_3OD) δ (ppm) 3.04 (dd, $J = 2.8$, 15.8 Hz, 1H), 3.44 (dd, $J = 6.4$, 15.8 Hz, 1H), 4.45 – 4.48 (m, 3H), 7.36 (d, $J = 8.0$ Hz; 2H) 7.49 (d, $J = 8.0$ Hz, 2H); ^{13}C NMR (100 MHz, CD_3OD) δ (ppm) 42.0, 43.6, 50.2, 118.4 (q, $J_{\text{ICF}} = 300.0$ Hz), 124.2, 130.0, 131.1, 141.2, 151.8, 162.4 (q, $J_{2\text{CF}} = 35.6$ Hz), 166.6, 172.9; ^{19}F NMR (375 MHz, CD_3OD) δ (ppm) -77.1; ESI-MS m/z 264 $[\text{M-TFA+H}]^+$, 281 $[\text{M-TFA+H}_2\text{O}]^+$. Found C, 44.44; H, 3.81; N, 10.91 %; $\text{C}_{14}\text{H}_{14}\text{F}_3\text{N}_3\text{O}_6$ requires C, 44.57; H, 3.74; N, 11.14 %.

***(S)*-(4-oxo-1-(*o*-tolylcarbamoyl)azetidine-2-carbonyl)glycine (6)**

Following GP2 compound **27** (29 mg, 0.70 mmol) yielded compound **6** as a white solid (21 mg, 99%). Mp 190 – 192°C; IR (film, cm^{-1}) 3356, 1778, 1737, 1690, 1674; $[\alpha]_{\text{D}}^{20} = -11$ ($c = 1.05$, CH_3OH); ^1H NMR (400 MHz, CD_3OD) δ (ppm) 2.29 (s, 3H), 3.14 (dd, $J = 2.9$, 15.8 Hz, 1H), 3.45 (dd, $J = 6.2$, 15.8 Hz, 1H), 3.93 (d, $J_{\text{AB}} = 17.8$ Hz, 1H), 4.08 (d, $J_{\text{AB}} = 17.8$ Hz, 1H), 4.63 (dd, $J = 2.9$, 6.2 Hz, 1H), 7.04 – 7.08 (m, 1H), 7.15 – 7.22 (m, 2H), 7.79 (d, $J = 8.0$ Hz, 1H); ^{13}C

NMR (100 MHz, CD₃OD) δ (ppm) 17.7, 41.9, 42.3, 51.5, 122.9, 126.0, 127.6, 129.9, 131.5, 136.4, 149.4, 167.9, 171.5, 172.5; ESI-MS m/z 609 [2M-H]⁻. Found C, 55.21; H, 4.99; N, 13.58 %; C₁₄H₁₅N₃O₅ requires C, 55.08; H, 4.95; N, 13.76 %.

***(S)*-3-(4-oxo-1-(*o*-tolylcarbamoyl)azetidine-2-carboxamido)propanoic acid (7)**

Following GP2 compound **28** (32 mg, 0.80 mmol) yielded compound **7** as a white solid (22 mg, 88%). Mp 161 – 163°C; IR (film, cm⁻¹) 3353, 1781, 1739, 1708, 1649; [α]_D²⁰ = -7 (c = 1.10, CH₃OH); ¹H NMR (400 MHz, CD₃OD) δ (ppm) 2.29 (s, 3H), 2.56 (t, J = 6.6 Hz, 2H), 3.08 (dd, J = 2.9, 15.8 Hz, 1H), 3.39 (dd, J = 6.1, 15.8 Hz, 1H), 3.45 – 3.57 (m, 2H), 4.52 (dd, J = 2.9, 6.1 Hz, 1H), 7.04 – 7.07 (m, 1H), 7.16 – 7.22 (m, 2H), 7.79 (d, J = 8.0 Hz, 1H); ¹³C NMR (100 MHz, CD₃OD) δ (ppm) 17.7, 34.4, 36.6, 42.1, 51.6, 122.9, 126.0, 127.6, 129.9, 131.5, 136.4, 149.3, 168.0, 171.0, 175.1; ESI-MS m/z 318 [M-H]⁻. Found C, 56.83; H, 5.38; N, 13.02 %; C₁₅H₁₇N₃O₅ requires C, 56.42; H, 5.37; N, 13.16 %.

***2*-(4-oxoazetidin-2-yl)acetic acid (8)**

Following GP2 compound **13** (130 mg, 0.59 mmol) yielded compound **8** as a white solid (75 mg, 99%). Mp 120 – 125°C; IR (nujol, cm⁻¹) 3230, 1752, 1695; ¹H NMR (400 MHz, CD₃OD) δ (ppm) 2.61 (dd, J = 7.7, 16.8 Hz, 1H), 2.65 (dd, J = 2.3, 14.8 Hz, 1H), 2.69 (dd, J = 5.8, 16.8 Hz, 1H), 3.10 (dd, J = 4.9, 14.8 Hz, 1H), 3.90 – 3.96 (m, 1H); ¹³C NMR (100 MHz, CD₃OD) δ (ppm) 40.5, 43.4, 45.3, 170.7, 174.6. Found C, 46.71; H, 5.59; N, 10.78 %; C₅H₇NO₃ requires C, 46.51; H, 5.46; N, 10.85 %.

2-(4-oxo-(o-tolylcarbamoyl)azetidin-2-yl) acetic acid (9)

Following GP2 compound **12** (88 mg, 0.25 mmol) yielded compound **9** as a white solid (65 mg, 99%). Mp 114 – 117°C; IR (film, cm^{-1}) 3344, 1766, 1708; ^1H NMR (400 MHz, $(\text{CD}_3)_2\text{CO}$) δ (ppm) 2.27 (s, 3H), 2.90 (dd, $J = 9.1, 16.7$ Hz, 1H), 3.08 (dd, $J = 2.9, 16.0$ Hz, 1H), 3.26 (dd, $J = 3.7, 16.7$ Hz, 1H), 3.42 (dd, $J = 5.7, 16.0$ Hz, 1H), 4.42 – 4.46 (m, 1H), 7.00 – 7.04 (m, 1H), 7.17 – 7.23 (m, 2H), 7.99 (d, $J = 8.1$ Hz, 1H), 8.55 (bs, 1H); ^{13}C NMR (100 MHz, $(\text{CD}_3)_2\text{CO}$) δ (ppm) 17.6, 36.6, 43.1, 48.4, 121.2, 124.7, 127.4, 127.7, 131.2, 136.9, 148.8, 168.4, 171.7; ESI-MS m/z 263 $[\text{M}+\text{H}]^+$, 285 $[\text{M}+\text{Na}]^+$, 547 $[\text{2M}+\text{Na}]^+$. Found C, 59.24; H, 5.56; N, 10.44 %; $\text{C}_{13}\text{H}_{14}\text{N}_2\text{O}_4$ requires C, 59.54; H, 5.38; N, 10.68 %.

Methyl 2-(4-oxo-1-(o-tolylcarbamoyl)azetidin-2-yl)acetate (10)

Compound **29** (77 mg, 0.54 mmol) was treated with K_2CO_3 (112 mg, 0.81 mmol) and commercial *o*-tolyl isocyanate (80 μL , 0.65 mmol) following GP1B. Chromatography ($\text{CH}_2\text{Cl}_2/\text{Et}_2\text{O}$ 90:10) yielded **10** as a waxy yellow solid (110 mg, 74%). IR (film, cm^{-1}) 3335, 1766, 1736, 1710; ^1H NMR (400 MHz, CDCl_3) δ (ppm) 2.30 (s, 3H), 2.74 (dd, $J = 9.0, 16.6$ Hz, 1H), 2.96 (dd, $J = 2.9, 16.6$ Hz, 1H), 3.35 (dd, $J = 4.6, 12.6$ Hz, 1H), 3.40 (dd, $J = 4.5, 12.6$ Hz, 1H), 3.73 (s, 3H), 4.43 – 4.49 (m, 1H), 7.03 – 7.06 (m, 1H), 7.18 – 7.23 (m, 2H), 7.92 (d, $J = 8.0$ Hz, 1H), 8.45 (bs, 1H); ^{13}C NMR (100 MHz, CDCl_3) δ (ppm) 17.6, 36.7, 42.7, 47.4, 52.0, 121.0, 124.5, 126.7, 127.5, 130.4, 135.2, 147.8, 166.8, 170.3; ESI-MS m/z 277 $[\text{M}+\text{H}]^+$. Found C, 61.12; H, 5.78; N, 9.98 %; $\text{C}_{14}\text{H}_{16}\text{N}_2\text{O}_4$ requires C, 60.86; H, 5.84; N, 10.14 %.

Ethyl 2-(4-oxo-1-(*o*-tolylcarbamoyl)azetidin-2-yl)acetate (11)

Compound **30** (65 mg, 0.41 mmol) was treated with K₂CO₃ (86 mg, 0.62 mmol) and commercial *o*-tolyl isocyanate (61 μ L, 0.49 mmol) following GP1B. Chromatography (CH₂Cl₂/Et₂O 80:20) yielded **11** as a white solid (110 mg, 81%). Mp 91 – 93°C; IR (film, cm⁻¹) 3340, 1761, 1730, 1714; ¹H NMR (400 MHz, CDCl₃) δ (ppm) 1.27 (t, *J* = 7.1 Hz, 3H), 2.30 (s, 3H), 2.74 (dd, *J* = 9.0, 16.5 Hz, 1H), 2.96 (dd, *J* = 2.8, 16.5 Hz, 1H), 3.33 (dd, *J* = 3.8, 16.6 Hz, 1H), 3.38 (dd, *J* = 5.7, 16.6 Hz, 1H), 4.18 (q, *J* = 7.1 Hz, 2H), 4.43 – 4.48 (m, 1H), 7.03 – 7.06 (m, 1H), 7.17 – 7.23 (m, 2H), 7.93 (d, *J* = 8.0 Hz, 1H), 8.45 (bs, 1H); ¹³C NMR (100 MHz, CDCl₃) δ (ppm) 14.1, 17.6, 36.8, 42.6, 47.5, 60.9, 120.9, 124.4, 126.7, 127.4, 130.4, 135.2, 147.8, 166.8, 169.8; ESI-MS *m/z* 291 [M+H]⁺, 603 [2M+Na]⁺. Found C, 62.13; H, 6.27; N, 9.41 %; C₁₅H₁₈N₂O₄ requires C, 62.06; H, 6.25; N, 9.65 %.

Benzyl 2-(4-oxo-(*o*-tolylcarbamoyl)azetidin-2-yl) acetate (12)

Compound **13** (75 mg, 0.34 mmol) was treated with K₂CO₃ (70 mg, 0.54 mmol) and commercial *o*-tolyl isocyanate (51 μ L, 0.41 mmol) following GP1B. Chromatography (CH₂Cl₂/Et₂O 90:10) yielded **12** as a white solid (110 mg, 74%). Mp 74 – 76°C; IR (film, cm⁻¹) 3338, 1767, 1733, 1713; ¹H NMR (400 MHz, CDCl₃) δ (ppm) 2.29 (s, 3H), 2.81 (dd, *J* = 8.8, 16.5 Hz, 1H), 2.95 (dd, *J* = 2.8, 16.5 Hz, 1H), 3.36 (dd, *J* = 6.0, 16.4 Hz, 1H), 3.37 (dd, *J* = 4.8, 16.4 Hz, 1H), 4.47 – 4.49 (m, 1H), 5.14 (d, *J*_{AB} = 12.6 Hz, 1H), 5.18 (d, *J*_{AB} = 12.6 Hz, 1H), 7.03 – 7.06 (m, 1H), 7.17 – 7.23 (m, 2H), 7.32 – 7.37 (m, 5H), 7.92 (d, *J* = 8.1 Hz, 1H), 8.42 (bs, 1H); ¹³C NMR (100 MHz, CDCl₃) δ (ppm) 17.7, 37.0, 42.6, 47.5, 66.8, 121.0, 124.4, 126.8, 127.5, 128.3, 128.4, 128.6, 130.4, 135.2, 135.3, 147.8, 166.7, 169.7; ESI-MS *m/z* 353 [M+H]⁺, 375 [M+Na]⁺,

727 [2M+Na]⁺. Found C, 68.43; H, 5.88; N, 7.80 %, C₂₀H₂₀N₂O₄ requires C, 68.17; H, 5.72; N, 7.95 %.

2-(1-(benzylcarbamoyl)-4-oxoazetidin-2-yl)acetic acid (14)

Following GP2 compound **33** (69 mg, 0.20 mmol) yielded compound **14** as a white solid (52 mg, 99%). Mp 100 – 103°C; IR (film, cm⁻¹) 3356, 1767, 1734, 1698; ¹H NMR (400 MHz, CDCl₃) δ (ppm) 2.65 (dd, *J* = 8.9, 16.8 Hz, 1H), 2.82 (dd, *J* = 2.3, 16.3 Hz, 1H), 3.21 – 3.29 (m, 2H), 4.31 – 4.34 (m, 1H), 4.37 – 4.47 (m, 2H), 6.92 (bt, *J* = 5.8 Hz, 1H), 7.23 – 7.32 (m, 5H), 7.50 (bs, 1H); ¹³C NMR (100 MHz, CDCl₃) δ (ppm) 36.8, 42.6, 43.5, 47.1, 127.5, 127.6, 128.6, 137.5, 150.6, 166.4, 173.7; ESI-MS *m/z* 261 [M-H]⁻. Found C, 59.41; H, 5.32; N, 10.59 %; C₁₃H₁₄N₂O₄ requires C, 59.54; H, 5.38; N, 10.68 %.

4-(2-(carboxymethyl)-4-oxoazetidine-1-carboxamidomethyl) benzenaminium trifluoroacetate (15)

Following GP3 compound **32** (14 mg, 0.37 mmol) and TFA (19.3 μL, 0.259 mmol, 7 equiv) yielded compound **15** (14 mg, 99%) as a yellow oil. IR (film, cm⁻¹) 3365, 1771, 1703, 1679; ¹H NMR (400 MHz, CD₃OD) δ (ppm) 2.75 (dd, *J* = 8.7, 16.6 Hz, 1H), 2.93 (dd, *J* = 3.0, 16.1 Hz, 1H), 3.11 (dd, *J* = 3.7, 16.6 Hz, 1H), 3.27 (dd, *J* = 5.8, 16.1 Hz, 1H), 4.28 – 4.33 (m, 1H), 4.44 – 4.46 (m, 2H), 7.29 (d, *J* = 8.4 Hz, 2H), 7.45 (d, *J* = 8.4 Hz, 2H); ¹³C NMR (100 MHz, CD₃OD) δ (ppm) 37.3, 43.2, 43.5, 48.6, 123.9, 130.1, 131.4, 141.2, 152.6, 168.1, 173.5; ¹⁹F NMR (375

MHz, CD₃OD) δ (ppm) -77.0; ESI-MS m/z 278 [M-TFA+H]⁺. Found C, 46.32; H, 3.98; N, 10.56 %; C₁₅H₁₆F₃N₃O₆ requires C, 46.04; H, 4.12; N, 10.74 %.

2-(4-oxo-(4-(3-*o*-tolylureidomethyl)phenylcarbamoyl)azetidin-2-yl) acetic acid (16)

Following GP2 compound **37** (79 mg, 0.158 mmol) yielded compound **16** as a white solid (64 mg, 99%). Mp 160 – 162°C; IR (film, cm⁻¹) 3319, 1774, 1707, 1629; ¹H NMR (400 MHz, CD₃CN) δ (ppm) 2,21 (s, 3H), 2.76 (dd, $J = 6.0, 16.5$ Hz, 1H), 2.93 (d, $J = 16.0$ Hz, 1H), 3.13 (d, $J = 16.5$ Hz, 1H), 3.28 (d, $J = 16.0$ Hz, 1H), 4.31 – 4.36 (m, 3H), 5.76 (bs, 1H), 6.68 (bs, 1H), 6.95 – 6.99 (m, 1H), 7.12 – 7.17 (m, 2H), 7.29 (d, $J = 8.9$ Hz, 2H), 7.44 (d, $J = 7.6$ Hz, 2H), 7.68 (d, $J = 7.8$ Hz, 1H), 8.45 (bs, 1H), 9.38 (bs, 1H); ¹³C NMR (100 MHz, CD₃OD) δ (ppm) 18.0, 37.3, 43.3, 44.2, 49.3, 121.1, 124.9, 125.4, 127.4, 129.0, 131.4, 131.7, 137.1, 137.5, 138.1, 149.7, 158.8, 168.6, 173.5; ESI-MS m/z 411 [M+H]⁺, 433 [M+Na]⁺, 821 [2M+H]⁺. Found C, 61.33; H, 5.35; N, 13.48 %; C₂₁H₂₂N₄O₅ requires C, 61.46; H, 5.40; N, 13.65 %.

2-(2-(4-oxo-(*o*-tolylcarbamoyl)azetidin-2-yl) acetamido) acetic acid (17)

Following GP2 compound **38** (85 mg, 0.208 mmol) yielded compound **17** as a white solid (66 mg, 99%). Mp 182 – 185°C; IR (film, cm⁻¹) 3300, 1764, 1720, 1649; ¹H NMR (400 MHz, CD₃OD) δ (ppm) 2.28 (s, 3H), 2.74 (dd, $J = 8.5, 14.8$ Hz, 1H), 3.08 – 3.16 (m, 2H), 3.29 – 3.37 (m, 1H), 3.88 (d, $J_{AB} = 17.4$ Hz, 1H), 3.94 (d, $J_{AB} = 17.4$ Hz, 1H), 4.39 – 4.47 (m, 1H), 7.03 – 7.07 (m, 1H), 7.16 – 7.22 (m, 2H), 7.81 (d, $J = 7.5$ Hz, 1H), 8.63 (bs, 1H) ¹³C NMR (100 MHz, CD₃OD) δ (ppm) 17.8, 38.8, 41.8, 43.1, 54.8, 122.9, 125.8, 127.6, 129.8, 131.5, 136.6, 150.0,

168.9, 172.3, 172.8; ESI-MS m/z 318 [M-H]⁻, 637 [2M-H]⁻. Found C, 56.13; H, 5.51; N, 12.98 %; C₁₅H₁₇N₃O₅ requires C, 56.42; H, 5.37; N, 13.16 %.

4-(2-(1-carboxymethyl-amidomethyl)-4-oxoazetidine-1-carboxamidomethyl) benzenaminium 2,2,2-trifluoroacetate (18)

Following GP3 compound **41** (19 mg, 0.044 mmol) and TFA (23 μL, 0.306 mmol, 7 equiv) yielded compound **18** (18.5 mg, 95%) as a yellow oil. IR (film, cm⁻¹) 3356, 1793, 1782, 1736, 1712, 1698; ¹H NMR (400 MHz, CD₃OD) δ (ppm) 2.68 (dd, $J = 8.3, 14.8$ Hz, 1H), 3.01 (dd, $J = 2.8, 16.1$ Hz, 1H), 3.07 (dd, $J = 4.0, 14.8$ Hz, 1H), 3.24 (dd, $J = 5.7, 16.1$ Hz, 1H), 3.85 – 3.94 (m, 2H), 4.31 – 4.38 (m, 1H), 4.43 (d, $J_{AB} = 15.8$ Hz, 1H), 4.48 (d, $J_{AB} = 15.8$ Hz, 1H), 7.33 (d, $J = 8.3$ Hz, 2H), 7.47 (d, $J = 8.3$ Hz, 2H); ¹³C NMR (100 MHz, CD₃OD) δ (ppm) 30.7, 38.9, 42.9, 43.5, 49.3, 123.8, 130.1, 131.8, 141.0, 152.6, 168.1, 172.3, 172.8; ¹⁹F NMR (375 MHz, CD₃OD) δ (ppm) -77.0; ESI-MS m/z 335 [M-TFA+H]⁺. Found C, 45.28; H, 4.51; N, 12.35 %; C₁₇H₁₉F₃N₄O₇ requires C, 45.54; H, 4.27; N, 12.50 %.

3-(2-(4-oxo-(o-tolylcarbamoyl)azetidin-2-yl)acetamido) propanoic acid (19)

Following GP2 compound **39** (61 mg, 0.144 mmol) yielded compound **19** as a white solid (47 mg, 99%). Mp 175 – 178°C; IR (film, cm⁻¹) 3300, 1769, 1700, 1638; ¹H NMR (400 MHz, CD₃OD) δ (ppm) 2.27 (s, 3H), 2.47 – 2.56 (m, 2H), 2.64 (dd, $J = 8.3, 14.7$ Hz, 1H), 3.00 – 3.08 (m, 2H), 3.29 – 3.36 (m, 1H), 3.40 – 3.48 (m, 2H), 4.38 – 4.43 (m, 1H), 7.03 – 7.06 (m, 1H), 7.16 – 7.22 (m, 2H), 7.81 (d, $J = 8.0$ Hz, 1H), 8.19 (bs, 1H); ¹³C NMR (100 MHz, CD₃OD) δ (ppm)

17.8, 34.5, 36.4, 39.3, 43.1, 49.8, 122.8, 125.8, 127.6, 129.7, 131.5, 136.6, 150.1, 159.4, 168.9, 172.1; ESI-MS m/z 332 [M-H]⁻, 665 [2M-H]⁻. Found C, 57.58; H, 5.80; N, 12.45 %; C₁₆H₁₉N₃O₅ requires C, 57.65; H, 5.75; N, 12.61 %.

4-((2-(2-((2-carboxyethyl)amino)-2-oxoethyl)-4-oxoazetidine-1-carboxamido)methyl)benzenaminium 2,2,2-trifluoroacetate (20)

Following GP3 compound **43** (19 mg, 0.044 mmol) was treated with TFA (56 μ L, 0.756 mmol, 18 equiv) yielding compound **20** (18 mg, 93%) as a yellow oil. IR (film, cm⁻¹) 3406, 1768, 1676, 1655, 1648; ¹H NMR (400 MHz, CD₃OD) δ (ppm) 2.49 (t, J = 6.7 Hz, 2H), 2.59 (dd, J = 8.1, 14.6 Hz, 1H), 2.92 – 2.98 (m, 2H), 3.24 (dd, J = 5.7, 16.1 Hz, 1H), 3.40 (t, J = 6.7 Hz, 2H), 4.28 – 4.33 (m, 1H), 4.43 (d, J_{AB} = 15.5 Hz, 1H), 4.48 (d, J_{AB} = 15.5 Hz, 1H), 7.32 (d, J = 8.3 Hz, 2H), 7.47 (d, J = 8.3 Hz, 2H); ¹³C NMR (100 MHz, CD₃OD) δ (ppm) 34.5, 36.3, 39.3, 42.9, 43.6, 49.4, 123.0, 129.7, 130.1, 139.7, 152.5, 168.1, 171.9, 175.2; ¹⁹F NMR (375 MHz, CD₃OD) δ (ppm) -77.0; ESI-MS m/z 461 [M-H]⁻. Found C, 46.89; H, 4.38; N, 12.00 %; C₁₈H₂₁F₃N₄O₇ requires C, 46.76; H, 4.58; N, 12.12 %.

(4-(2-(2-((2-carboxyethyl)amino)-2-oxoethyl)-4-oxoazetidine-1-carboxamido)phenyl)methanaminium 2,2,2-trifluoroacetate (21)

Following GP3 compound **46** (60 mg, 0.13 mmol) was treated with TFA (174 μ L, 2.34 mmol, 18 equiv) yielding compound **21** (51 mg, 87%) as a white solid. Mp 121 – 124°C; IR (film, cm⁻¹) 3060, 1781, 1753, 1699, 1685, 1655; ¹H NMR (400 MHz, CD₃OD) δ (ppm) 2.52 (t, J = 6.7 Hz,

2H), 2.66 (dd, $J = 7.9, 14.9$ Hz, 1H), 2.98 – 3.04 (m, 2H), 3.33 – 3.35 (m, 1H), 3.43 (t, $J = 6.7$ Hz, 2H), 4.08 (s, 2H), 4.39 – 4.42 (m, 1H), 7.41 (d, $J = 8.5$ Hz, 2H), 7.59 (d, $J = 8.5$ Hz, 2H), 8.88 (bs, 1H); ^{13}C NMR (100 MHz, CD_3OD) δ (ppm) 34.6, 36.4, 39.3, 43.1, 43.9, 49.8, 121.3, 121.4, 129.9, 130.9, 139.6, 149.5, 168.5, 172.1, 175.2; ^{19}F NMR (375 MHz, CD_3OD) δ (ppm) -77.0; ESI-MS m/z 461 [M-H]. Found C, 46.58; H, 4.76; N, 11.84 %; $\text{C}_{18}\text{H}_{21}\text{F}_3\text{N}_4\text{O}_7$ requires C, 46.76; H, 4.58; N, 12.12 %.

***(S)*-Benzyl 1-(4-*tert*-butoxycarbonylamino benzyl carbamoyl)-4-oxoazetidine-2-carboxylate (24)**

Compound **22** (35 mg, 0.17 mmol) was treated with NaHMDSA (375 μL , 0.375 mmol) and isocyanate **23** (64 mg, 0.26 mmol) following GP1A. Flash chromatography ($\text{CH}_2\text{Cl}_2/\text{Et}_2\text{O}$ 95:5) yielded **24** as a colorless oil (69 mg, 37%). IR (film, cm^{-1}) 3358, 1780, 1744, 1731, 1709; $[\alpha]_{\text{D}}^{20} = -0.4$ ($c = 0.93$, CH_2Cl_2); ^1H NMR (400 MHz, CDCl_3) δ (ppm) 1.51 (s, 9H), 3.01 (dd, $J = 2.8, 15.6$ Hz, 1H), 3.30 (dd, $J = 6.2, 15.6$ Hz, 1H), 4.38 (dd, $J = 6.0, 14.8$ Hz, 1H), 4.45 (dd, $J = 6.0, 14.8$ Hz, 1H), 4.52 (dd, $J = 2.8, 6.2$ Hz, 1H), 5.22 (d, $J_{AB} = 12.2$ Hz, 1H), 5.27 (d, $J_{AB} = 12.2$ Hz, 1H), 6.56 (s, 1H), 6.67 (bt, $J = 6.0$ Hz, 1H), 7.19 – 7.21 (m, 2H), 7.27 – 7.39 (m, 7H); ^{13}C NMR (100 MHz, CDCl_3) δ (ppm) 28.2, 41.0, 43.3, 48.7, 67.6, 80.4, 118.7, 128.2, 128.3, 128.5, 128.6, 129.9, 132.0, 134.7, 137.8, 149.3, 152.6, 164.6, 169.0; ESI-MS m/z 471 $[\text{M} + \text{H}_2\text{O}]^+$, 476 $[\text{M} + \text{Na}]^+$.

***(S)*-1-(4-*tert*-butoxycarbonylamino benzyl carbamoyl)-4-oxoazetidine-2-carboxylic acid (25)**

Following GP2 compound **24** (51 mg, 0.11 mmol) yielded compound **25** as a waxy white solid (35 mg, 88%). IR (film, cm^{-1}) 3363, 1770, 1699, 1694, 1692; $[\alpha]_{\text{D}}^{20} = -0.5$ ($c = 0.64$, CH_3OH); ^1H NMR (400 MHz, CD_3OD) δ (ppm) 1.50 (s, 9H), 2.90 (dd, $J = 2.8, 15.6$ Hz, 1H), 3.27 (dd, $J = 6.4, 15.6$ Hz, 1H), 4.31 – 4.41 (m, 3H), 7.22 (d, $J = 8.4$ Hz, 2H), 7.35 (d, $J = 8.4$ Hz, 2H); ^{13}C NMR (100 MHz, CD_3OD) δ (ppm) 28.7, 41.9, 43.9, 49.2, 80.8, 119.9, 128.9, 130.1, 133.8, 139.7, 150.7, 151.7, 155.2, 166.6; ESI-MS m/z 362 $[\text{M}-\text{H}]^-$.

***(S)*-Benzyl 4-oxo-(*o*-tolylcarbamoyl)azetidine-2-carboxylate (26)**

Compound **22** (103 mg, 0.5 mmol) was treated with K_2CO_3 (104 mg, 0.75 mmol) and commercial *o*-tolyl isocyanate (74 μL , 0.6 mmol) following GP1B. Flash chromatography (Cyclohexane/AcOEt 70:30) yielded **26** as a light brown oil (126 mg, 75%). IR (film, cm^{-1}) 3348, 1776, 1751, 1718; $[\alpha]_{\text{D}}^{20} = -9$ ($c = 1.15$, CH_2Cl_2); ^1H NMR (400 MHz, CDCl_3) δ (ppm) 2.30 (s, 3H), 3.12 (dd, $J = 2.8, 15.8$ Hz, 1H), 3.42 (dd, $J = 6.2, 15.8$ Hz, 1H), 4.62 (dd, $J = 2.8, 6.2$ Hz, 1H), 5.25 (d, $J_{\text{AB}} = 12.2$ Hz, 1H), 5.30 (d, $J_{\text{AB}} = 12.2$ Hz, 1H), 7.04 – 7.08 (m, 1H), 7.18 – 7.21 (m, 2H), 7.35 – 7.38 (m, 5H), 7.93 (d, $J = 8.1$ Hz, 1H), 8.28 (bs, 1H); ^{13}C NMR (100 MHz, CDCl_3) δ (ppm) 17.3, 41.0, 48.8, 67.5, 120.9, 124.4, 126.6, 127.4, 128.1, 128.4, 128.4, 130.2, 134.6, 134.9, 146.6, 165.1, 168.7; ESI-MS m/z 339 $[\text{M}+\text{H}]^+$, 361 $[\text{M}+\text{Na}]^+$, 699 $[2\text{M}+\text{Na}]^+$.

***Benzyl (S)*-(4-oxo-1-(*o*-tolylcarbamoyl)azetidine-2-carbonyl)glycinate (27)**

Carboxylic acid **4** (40 mg, 0.16 mmol, 1 equiv) was dissolved in CH_2Cl_2 (1.6 mL) under nitrogen and oxalyl chloride (21 μL , 0.24 mmol, 1.5 equiv) was added dropwise. The mixture was stirred

at room temperature for 1.5 h and glycine benzylester hydrochloride (32 mg, 0.16 mmol, 1 equiv) was then added, followed by the addition of TEA (112 μ L, 0.8 mmol, 5 equiv) in a cold-water bath and DMAP (4 mg, 0.032 mmol, 0.2 equiv). The mixture was warmed to rt and left under stirring overnight. After complete consumption of the starting material (16 h) the mixture was quenched with a saturated solution of NH_4Cl and extracted with CH_2Cl_2 (3 x 10mL). The collected organic layers were dried on Na_2SO_4 , filtered and evaporated in vacuum. Purification by column chromatography (cyclohexane/AcOEt 60:40) afforded compound **27** (32 mg, 51%) as a white waxy solid.

IR (film, cm^{-1}) 3337, 1774, 1750, 1719, 1687; $[\alpha]_{\text{D}}^{20} = -12$ ($c = 1.00$, CH_2Cl_2); ^1H NMR (400 MHz, CDCl_3) δ (ppm) 2.30 (s, 3H), 3.32 (dd, $J = 6.4, 16.4$ Hz, 1H), 3.53 (dd, $J = 3.2, 16.4$ Hz, 1H), 4.07 – 4.18 (m, 2H), 4.70 (dd, $J = 3.2, 6.4$ Hz, 1H), 5.16 (d, $J_{AB} = 12.4$ Hz, 1H), 5.20 (d, $J_{AB} = 12.4$ Hz, 1H), 7.06 – 7.10 (m, 1H), 7.19 – 7.24 (m, 2H), 7.31 – 7.35 (m, 5H), 7.88 (d, $J = 8.0$ Hz, 1H), 7.99 (bt, $J = 5.0$ Hz, 1H), 8.48 (bs, 1H); ^{13}C NMR (100 MHz, CDCl_3) δ (ppm) 17.6, 40.4, 41.6, 51.7, 67.2, 121.4, 125.0, 126.8, 128.0, 128.3, 128.5, 128.6, 130.5, 134.6, 135.0, 148.9, 166.8, 167.9, 169.0; ESI-MS m/z 396 $[\text{M}+\text{H}]^+$, 418 $[\text{M}+\text{Na}]^+$.

Benzyl (S)-3-(4-oxo-1-(o-tolylcarbonyl)azetidine-2-carboxamido)propanoate (28)

Carboxylic acid **4** (40 mg, 0.16 mmol, 1 equiv) was dissolved in CH_2Cl_2 (1.6 mL) under nitrogen and oxalyl chloride (16 μ L, 0.19 mmol, 1.2 equiv) was added dropwise. The mixture was stirred at room temperature for 1.5 h and β -alanine benzylester *p*-toluenesulfonate salt (56 mg, 0.16 mmol, 1 equiv) was then added, followed by the addition of TEA (90 μ L, 0.64 mmol, 4 equiv) in a cold-water bath and DMAP (4 mg, 0.032 mmol, 0.2 equiv). The mixture was warmed to rt and

left under stirring overnight. After complete consumption of the starting material (16 h) the mixture was quenched with a saturated solution of NH_4Cl and extracted with CH_2Cl_2 (3x10 mL). The collected organic layers were dried on Na_2SO_4 , filtered and evaporated in vacuum. Purification by column chromatography (cyclohexane/AcOEt 60:40) afforded compound **28** (35 mg, 54%) as a white waxy solid. IR (film, cm^{-1}) 3340, 1774, 1729, 1686, 1683; $[\alpha]_{\text{D}}^{20} = -11$ (c = 1.00, CH_2Cl_2); ^1H NMR (400 MHz, CDCl_3) δ (ppm) 2.30 (s, 3H), 2.63 (t, $J = 6.3$ Hz, 2H), 3.28 (dd, $J = 6.3, 16.3$ Hz, 1H), 3.48 (dd, $J = 3.2, 16.3$ Hz, 1H), 3.54 – 3.67 (m, 2H), 4.55 (dd, $J = 3.2, 6.3$ Hz, 1H), 5.12 (s, 2H), 7.05 – 7.09 (m, 1H), 7.19 – 7.22 (m, 2H), 7.30 – 7.35 (m, 5H), 7.71 (bs, 1H), 7.88 (d, $J = 8.8$ Hz, 1H), 8.46 (bs, 1H); ^{13}C NMR (100 MHz, CDCl_3) δ (ppm) 17.6, 33.9, 35.3, 40.4, 51.8, 66.5, 121.4, 125.0, 126.8, 128.0, 128.2, 128.3, 128.5, 130.5, 134.7, 135.6, 148.7, 166.9, 167.5, 171.6; ESI-MS m/z 410 $[\text{M}+\text{H}]^+$, 432 $[\text{M}+\text{Na}]^+$.

Methyl 2-(4-oxoazetidin-2-yl)acetate (29)

Zn powder (2.018 g, 31.04 mmol, 7.2 equiv) was suspended in THF (9.7 mL) under nitrogen followed by TMSCl (196 μL , 1.552 mmol, 0.1 equiv) addition. After 30 min of stirring the temperature was raised to $30 \div 35$ °C and a solution of methyl bromoacetate (1.47 mL, 15.52 mmol, 3.6 equiv) in THF (19.4 mL) was added dropwise in 30 min. After 30 min of stirring the mixture was cooled to rt and decanted, providing a limpid grey supernatant that was added dropwise to a solution of commercially available 4-acetoxy-azetidin-2-one (500 mg, 3.88 mmol, 1 equiv) in anhydrous THF (22 mL) at 0°C. The mixture was stirred at rt for 3 h, quenched with ice and a saturated Seignette salt solution and extracted with AcOEt (5x50 mL). The organic

layers were dried on Na₂SO₄, filtered and concentrated in vacuum. Flash-chromatography (cyclohexane/AcOEt 70:30 to AcOEt 100%) yielded ester **29** (332 mg, 60%) as a yellow solid.

Mp 60 – 65°C; IR (film, cm⁻¹) 3390, 1760, 1730; ¹H NMR (400 MHz, CDCl₃) δ (ppm) 2.63 (dd, *J* = 8.6, 16.7 Hz, 1H), 2.69 – 2.73 (m 1H), 2.74 (dd, *J* = 5.0, 16.7 Hz, 1H), 3.20 (ddd, *J* = 2.2, 5.0, 15.2 Hz, 1H), 3.70 (s, 3H), 3.96 – 4.02 (m, 1H), 6.77 (bs, 1H); ¹³C NMR (100 MHz, CDCl₃) δ (ppm) 39.2, 43.0, 44.6, 52.0, 169.0, 171.0; ESI-MS *m/z* 144 [M+H]⁺.

Ethyl 2-(4-oxoazetidin-2-yl)acetate (30)

Following the procedure reported for **29**, commercially available 4-acetoxy-azetidin-2-one (500 mg, 3.88 mmol, 1 equiv) was treated with ethyl bromoacetate (1.72 mL, 15.52 mmol, 3.6 equiv). Purification by column chromatography (CH₂Cl₂/acetone 80:20) yielded compound **30** (390 mg, 64%) as a waxy yellow solid. IR (film, cm⁻¹) 3224, 1731, 1725; ¹H NMR (400 MHz, CDCl₃) δ (ppm) 1.27 (t, *J* = 7.2 Hz, 3H), 2.58 (dd, *J* = 9.0, 16.6 Hz, 1H), 2.66 (dd, *J* = 1.3, 14.9 Hz, 1H), 2.73 (dd, *J* = 4.6, 16.6 Hz, 1H), 3.16 (ddd, *J* = 2.2, 4.8, 14.9 Hz, 1H), 3.92 – 3.95 (m, 1H), 4.17 (q, *J* = 7.1 Hz, 2H), 6.14 (bs, 1H); ¹³C NMR (100 MHz, CDCl₃) δ (ppm) 14.2, 39.9, 43.4, 43.8, 61.0, 167.0, 170.9; ESI-MS *m/z* 158 [M+H]⁺, 180 [M+Na]⁺.

Benzyl 2-(1-(4-tert-butoxycarbonylaminobenzylcarbamoyl)-4-oxoazetidin-2-yl acetate (31)

Compound **13** (57 mg, 0.26 mmol) was treated with NaHMDSA (325 μL, 0.325 mmol) and isocyanate **23** (97 mg, 0.39 mmol) following GP1A. Chromatography (CH₂Cl₂ /Et₂O 95:5) yielded **31** as a colorless oil (75 mg, 62%). IR (film, cm⁻¹) 3365, 1769, 1730, 1703, 1697; ¹H

NMR (400 MHz, CDCl₃) δ (ppm) 1.51 (s, 9H), 2.71 (dd, $J = 9.0, 16.5$ Hz, 1H), 2.84 (dd, $J = 2.9, 16.2$ Hz, 1H), 3.26 (dd, $J = 5.6, 16.2$ Hz, 1H), 3.34 (dd, $J = 4.0, 16.5$ Hz, 1H), 4.31 – 4.43 (m, 3H), 5.12 (d, $J_{AB} = 12.2$ Hz, 1H), 5.16 (d, $J_{AB} = 12.2$ Hz, 1H), 6.46 (bs, 1H), 6.77 (bt, $J = 5.7$ Hz) 7.20 – 7.22 (m, 2H), 7.30 – 7.39 (m, 7H); ¹³C NMR (100 MHz, CDCl₃) δ (ppm) 28.2, 37.0, 42.5, 43.0, 47.1, 66.6, 80.5, 118.7, 128.2, 128.3, 128.5, 132.2, 135.3, 137.8, 150.2, 152.6, 166.1, 169.7; ESI-MS m/z 468 [M+H]⁺, 485 [M+H₂O]⁺, 490 [M+Na]⁺, 506 [M+K]⁺.

2-(1-(4-tert-butoxycarbonylaminobenzylcarbamoyl)-4-oxoazetidin-2-yl acetic acid (32)

Following GP2 compound **31** (39 mg, 0.80 mmol) yielded compound **32** as a white solid (30 mg, 99%). Mp 78 – 81°C; IR (film, cm⁻¹) 3355, 1769, 1731, 1707, 1695; ¹H NMR (400 MHz, CD₃OD) δ (ppm) 1.51 (s, 9H), 2.73 (dd, $J = 8.9, 16.5$ Hz, 1H), 2.91 (dd, $J = 2.6, 16.0$ Hz, 1H), 3.13 (dd, $J = 2.4, 16.5$ Hz, 1H), 3.28 (dd, $J = 5.6, 16.0$ Hz, 1H), 4.28 – 4.31 (m, 1H), 4.34 – 4.36 (m, 2H), 7.21 (d, $J = 8.4$ Hz; 2H), 7.35 (d, $J = 8.3$ Hz; 2H); ¹³C NMR (100 MHz, CD₃OD) δ (ppm) 28.7, 37.3, 43.2, 43.7, 43.8, 80.8, 119.9, 128.9, 133.9, 139.7, 152.4, 155.2, 168.1, 173.5; ESI-MS m/z 376 [M-H]⁻.

Benzyl 2-(1-(benzylcarbamoyl)-4-oxoazetidin-2-yl)acetate (33)

Compound **13** (80 mg, 0.37 mmol) was treated with K₂CO₃ (77 mg, 0.56 mmol) and commercial benzyl isocyanate (54 μ L, 0.44 mmol) following GP1B. Chromatography (CH₂Cl₂/Et₂O 90:10) yielded **33** as a light yellow oil (96 mg, 74%). IR (film, cm⁻¹) 3367, 1767, 1732, 1694; ¹H NMR (400 MHz, CDCl₃) δ (ppm) 2.69 (dd, $J = 9.0, 16.5$ Hz, 1H), 2.81 (dd, $J = 2.9, 16.2$ Hz, 1H), 3.22

(dd, $J = 5.6, 16.2$ Hz, 1H), 3.30 (dd, $J = 4.0, 16.5$ Hz, 1H), 4.31 – 4.36 (m, 1H), 4.37 – 4.46 (m, 2H), 5.09 (d, $J_{AB} = 12.3$ Hz, 1H), 5.13 (d, $J_{AB} = 12.3$ Hz, 1H), 6.82 (bt, $J = 5.6$ Hz, 1H), 7.22 – 7.36 (m, 10H); ^{13}C NMR (100 MHz, CDCl_3) δ (ppm) 37.0, 42.4, 43.4, 47.0, 66.6, 127.4, 127.5, 128.2, 128.3, 128.5, 128.6, 135.3, 137.7, 150.3, 166.1, 169.6; ESI-MS m/z 353 $[\text{M}+\text{H}]^+$.

4-(2-(2-(benzyloxy)-2-oxoethyl)-4-oxoazetidine-carboxamido)phenyl methanaminium 2,2,2-trifluoroacetate (36)

Following GP3 compound **35** (133 mg, 0.284 mmol) was treated with TFA (322 μL , 4.32 mmol, 15.2 equiv) yielding compound **36** (136 mg, 99%) as a waxy white solid. IR (film, cm^{-1}) 3336, 1771, 1704, 1680; ^1H NMR (400 MHz, CDCl_3) δ (ppm) 2.81 (dd, $J = 8.6, 16.5$ Hz, 1H), 2.96 (dd, $J = 2.6, 16.4$ Hz, 1H), 3.30 – 3.38 (m, 2H), 4.25 (bs, 2H), 4.44 – 4.50 (m, 1H), 5.16 (s, 2H), 7.21 – 7.23 (m, 2H), 7.33 – 7.35 (m, 5H), 7.39 – 7.41 (m, 2H), 8.45 (bs, 1H), 8.77 (bs, 3H); ^{13}C NMR (100 MHz, CDCl_3) δ (ppm) 36.7, 42.5, 43.0, 47.6, 66.8, 120.4, 127.9, 128.2, 128.4, 128.5, 129.8, 135.2, 137.3, 147.9, 166.8, 169.9; ESI-MS m/z 351 $[\text{M}-\text{TFA}-\text{NH}_3+\text{H}]^+$, 735 $[\text{M}-2\text{TFA}+\text{H}]^+$.

Benzyl 2-(4-oxo-(4-(3-*o*-tolylureidomethyl)phenylcarbamoyle)azetidin-2-yl) acetate (37)

To a solution of **36** (136 mg, 0.28 mmol, 1 equiv) in THF (1.6 mL) under nitrogen was added dropwise TEA (43 μL , 0.31 mmol, 1.1 equiv) and left under stirring. After 30 min the mixture was cooled to 0°C and a solution of *o*-tolyl-isocyanate (38 μL , 0.31 mmol, 1.1 equiv) in THF (0.8 mL) was added. When TLC indicated the complete consumption of the starting material (1.5

h), the mixture was concentrated under vacuum and the resulting crude was purified by flash-chromatography (CH₂Cl₂/AcOEt, 90:10 to 70:30) to afford **37** as a white solid (79 mg, 56%). Mp 184 – 187°C; IR (film, cm⁻¹) 3319, 1771 1712; ¹H NMR (400 MHz, CDCl₃) δ (ppm) 2.25 (s, 3H), 2.79 (dd, *J* = 8.8, 16.5 Hz, 1H), 2.94 (dd, *J* = 2.6, 16.3 Hz, 1H), 3.32 – 3.37 (m, 2H), 4.40 (bs, 2H), 4.42 – 4.47 (m, 1H), 5.15 (s, 2H), 6.21 (bs, 1H), 7.13 – 7.41 (m, 13H), 8.41 (bs, 1H); ¹³C NMR (100 MHz, CDCl₃) δ (ppm) 17.8, 36.8, 42.7, 44.0, 47.5, 66.8, 119.9, 125.7, 126.3, 127.2, 128.2, 128.3, 128.4, 128.5, 128.6, 131.1, 132.2, 134.9, 135.3, 136.1, 156.6, 166.6, 169.6, 174.2; ESI-MS *m/z* 501 [M+H]⁺, 523 [M+Na]⁺, 1001 [2M+H]⁺.

Benzyl 2-(2-(4-oxo-(o-tolylcarbamoyl)azetidin-2-yl) acetamido) acetate (38)

Carboxylic acid **9** (98 mg, 0.374 mmol, 1 equiv) was dissolved in CH₂Cl₂ (5.4 mL) under nitrogen. 1-Ethyl-3-(3-dimethylaminopropyl) carbodiimide (EDC) (72 mg, 0.374 mmol, 1 equiv) was then added at 0°C. It was followed by the dropwise addition of a previously prepared solution of glycine benzyl ester *p*-toluenesulfonate salt (189 mg, 561 μmol, 1.5 equiv) and TEA (84 μL, 0.598 mmol, 1.6 equiv) in CH₂Cl₂ (4.7 mL). After addition of DMAP (46 mg, 0.374 mmol, 1 equiv), the solution was warmed to rt and left under stirring overnight. After complete consumption of the starting material (16 h) the mixture was quenched with H₂O and extracted with CH₂Cl₂ (3x10 mL). The collected organic layers were dried on Na₂SO₄ and filtered. The organic layer was concentrated in vacuum and purified by flash-chromatography (CH₂Cl₂/CH₃CN 95:5 to 80:20) yielding compound **38** (85 mg, 56%) as a light yellow solid. Mp 174 – 176°C; IR (film, cm⁻¹) 3321, 1767, 1723, 1708, 1645; ¹H NMR (400 MHz, CDCl₃) δ (ppm) 2.30 (s, 3H), 2.78 (dd, *J* = 7.9, 14.9 Hz, 1H), 3.14 – 3.21 (m, 2H), 3.34 (dd, *J* = 5.4, 16.4

Hz, 1H), 4.02 (dd, $J = 4.8, 18.4$ Hz, 1H), 4.11 (dd, $J = 5.4, 18.4$ Hz, 1H), 4.43 – 4.48 (m, 1H), 5.16 (s, 2H), 6.43 (bt, $J = 5.8$ Hz, 1H), 7.04 – 7.07 (m, 1H), 7.18 – 7.23 (m, 2H), 7.32 – 7.39 (m, 5H), 7.89 (d, $J = 7.9$ Hz, 1H), 8.51 (bs, 1H); ^{13}C NMR (100 MHz, CDCl_3) δ (ppm) 17.7, 38.2, 41.3, 42.6, 48.4, 67.2, 121.2, 124.6, 126.7, 127.8, 128.4, 128.5, 128.6, 130.5, 135.0, 135.1, 148.5, 167.2, 169.2, 169.4; ESI-MS m/z 410 $[\text{M}+\text{H}]^+$, 432 $[\text{M}+\text{Na}]^+$.

Benzyl 3-(2-(4-oxo-(o-tolylcarbamoyl)azetidin-2-yl)acetamido) propanoate (39)

Carboxylic acid **9** (63 mg, 0.240 mmol, 1 equiv) was dissolved in CH_2Cl_2 (3.47 mL) under nitrogen. EDC (46 mg, 0.240 mmol, 1 equiv) was then added at 0°C . It was followed by the dropwise addition of a previously prepared solution of β -alanine benzylester *p*-toluenesulfonate salt (127 mg, 0.360 mmol, 1.5 equiv) and TEA (54 μL , 0.384 mmol, 1.6 equiv) in CH_2Cl_2 (3 mL). After addition of DMAP (29 mg, 0.240 mmol, 1 equiv), the solution was warmed to rt and left under stirring overnight. After complete consumption of the starting material (16 h) the mixture was quenched with H_2O and extracted with CH_2Cl_2 (3x10 mL). The collected organic layers were dried on Na_2SO_4 and filtered. The organic layer was concentrated in vacuum and purified by flash-chromatography ($\text{CH}_2\text{Cl}_2/\text{AcOEt}$ 80:20 to 70:30) yielding compound **39** (61 mg, 60%) as a white waxy solid.

IR (film, cm^{-1}) 3334, 1765, 1732, 1712, 1656; ^1H NMR (400 MHz, CDCl_3) δ (ppm) 2.29 (s, 3H), 2.51 – 2.64 (m, 3H), 3.07 (dd, $J = 3.8, 15.1$ Hz, 1H), 3.12 (dd, $J = 3.0, 16.4$ Hz, 1H), 3.32 (dd, $J = 5.6, 16.4$ Hz, 1H), 3.48 – 3.57 (m, 2H), 4.36 – 4.41 (m, 1H), 5.06 (d, $J_{\text{AB}} = 12.4$ Hz, 1H), 5.10 (d, $J_{\text{AB}} = 12.4$ Hz, 1H), 6.44 (bs, 1H) 7.02 – 7.06 (m, 1H), 7.17 – 7.22 (m, 2H), 7.31 – 7.39 (m, 5H), 7.92 (d, $J = 7.9$ Hz, 1H), 8.50 (bs, 1H); ^{13}C NMR (100 MHz, CDCl_3) δ (ppm) 17.6, 33.8,

34.8, 38.4, 42.6, 48.3, 66.4, 120.9, 124.4, 126.7, 127.5, 128.1, 128.3, 128.5, 130.4, 135.1, 135.5, 148.2, 167.2, 168.8, 172.0; ESI-MS m/z 424 $[M+H]^+$, 446 $[M+Na]^+$.

Benzyl 2-(2-(4-tert-butoxycarbonylamino benzyl carbamoyl)-4-oxoazetidin-2-yl acetamido) acetate (40)

Carboxylic acid **32** (27 mg, 0.72 mmol, 1 equiv) was dissolved in a mixture of CH_2Cl_2 (0.85 mL) and CH_3CN (0.17 mL) under nitrogen. Dicyclohexylcarbodiimide (DCC) (16 mg, 0.79 mmol, 1.1 equiv) was then added at 0°C. It was followed by the dropwise addition of a previously prepared solution of glycine benzylester *p*-toluenesulfonate salt (38 mg, 0.108 mmol, 1.5 equiv) and TEA (16 μ L, 0.115 mmol, 1.6 equiv) in CH_2Cl_2 (0.9 mL). After addition of catalytic DMAP (2 mg, 0.014 mmol, 0.2 equiv), the solution was warmed to rt and left under stirring overnight. After complete consumption of the starting material (16 h) the mixture was quenched with H_2O and extracted with CH_2Cl_2 (3x10 mL). The collected organic layers were dried on Na_2SO_4 and filtered. The crude was suspended in AcOEt and the solid residual dicyclohexylurea was eliminated by filtration. The organic layer was concentrated in vacuum and purified by flash-chromatography (CH_2Cl_2/CH_3CN 95:5 to 80:20) yielding compound **40** (27 mg, 72%) as a light yellow solid. Mp 64 – 66°C; IR (film, cm^{-1}) 3355, 1766, 1724, 1707, 1691, 1671; 1H NMR (400 MHz, $CDCl_3$) δ (ppm) 1.50 (s, 9H), 2.69 (dd, $J = 8.0, 15.0$ Hz, 1H), 3.05 (dd, $J = 3.0, 16.4$ Hz, 1H), 3.10 (dd, $J = 3.8, 15.0$ Hz, 1H), 3.22 (dd, $J = 5.6, 16.4$ Hz, 1H), 3.99 (dd, $J_{AB} = 5.4, 18.2$ Hz, 1H), 4.05 (dd, $J_{AB} = 5.5, 18.2$ Hz; 1H), 4.30 – 4.41 (m, 3H), 5.16 (s, 2H), 6.54 (bs, 1H), 6.66 (bs, 1H), 6.90 (bt, $J = 5.9$ Hz, 1H), 7.17 – 7.22 (m, 2H), 7.28 – 7.39 (m, 7H); ^{13}C NMR (100 MHz, $CDCl_3$) δ (ppm) 28.3, 38.4, 41.3, 42.6, 43.1, 48.0, 67.2, 80.6, 118.8, 128.3, 128.4, 128.5,

128.6, 132.2, 135.1, 137.8, 150.9, 152.7, 166.7, 169.3, 169.5; ESI-MS m/z 525 $[M+H]^+$, 542 $[M+H_2O]^+$, 547 $[M+Na]^+$, 563 $[M+K]^+$.

2-(2-(1-(4-tert-butoxycarbonylamino)benzylcarbamoyl)-4-oxoazetidin-2-yl) acetamido) acetic acid (41)

Following GP2 compound **40** (22 mg, 0.042 mmol) yielded compound **41** as a white solid (18 mg, 99%). Mp 100 – 103°C; IR (film, cm^{-1}) 3350, 1768, 1717, 1694, 1682; 1H NMR (400 MHz, CD_3OD) δ (ppm) 1.51 (s, 9H), 2.65 (dd, $J = 8.6, 14.6$ Hz, 1H), 2.95 – 3.03 (m, 1H), 3.05 – 3.14 (m, 1H), 3.24 (dd, $J = 5.4, 16.0$ Hz, 1H), 3.86 (d, $J_{AB} = 19.9$ Hz, 1H), 3.91 (d, $J_{AB} = 19.9$ Hz, 1H), 4.27 – 4.39 (m, 3H), 7.21 (d, $J = 7.8$ Hz, 2H), 7.35 (d, $J = 7.8$ Hz, 2H), 8.86 (bs, 1H); ^{13}C NMR (100 MHz, $CDCl_3$) δ (ppm) 28.7, 30.7, 39.1, 43.0, 43.8, 49.3, 80.8, 119.9, 129.0, 134.0, 139.8, 152.5, 155.3, 168.1, 172.3, 173.0; ESI-MS m/z 435 $[M+H]^+$, 457 $[M+Na]^+$.

Benzyl 3-(2-(1-((4-((tert-butoxycarbonyl)amino)benzyl)carbamoyl)-4-oxoazetidin-2-yl) acetamido)propanoate (42)

Carboxylic acid **32** (62 mg, 0.164 mmol, 1 equiv) was dissolved in a mixture of CH_2Cl_2 (1.85 mL) and CH_3CN (0.36 mL) under nitrogen. DCC (32 mg, 0.181 mmol, 1.1 equiv) was then added at 0°C. It was followed by the dropwise addition of a previously prepared solution of beta alanine benzylester *p*-toluenesulfonate salt (86 mg, 0.246 mmol, 1.5 equiv) and TEA (37 μ L, 0.262 mmol, 1.6 equiv) in CH_2Cl_2 (2 mL). After addition of catalytic DMAP (4 mg, 0.033 mmol, 0.2 equiv), the solution was warmed to rt and left under stirring overnight. After complete

consumption of the starting material (16 h) the mixture was quenched with H₂O and extracted with CH₂Cl₂ (3x10 mL). The collected organic layers were dried on Na₂SO₄ and filtered. The crude was suspended in AcOEt and the solid residual dicyclohexylurea was eliminated by filtration. The organic layer was concentrated in vacuum and purified by flash-chromatography (AcOEt/CH₂Cl₂ 70:30) yielding compound **42** (65 mg, 74%) as a light yellow waxy solid. IR (film, cm⁻¹) 3434, 1767, 1726, 1698, 1665; ¹H NMR (400 MHz, CDCl₃) δ (ppm) 1.50 (s, 9H), 2.49 – 2.61 (m, 3H), 2.96 – 3.02 (m, 2H), 3.19 (dd, *J* = 5.6, 16.3 Hz, 1H), 3.41 – 3.55 (m, 2H), 4.25 – 4.28 (m, 1H), 4.32 (dd, *J* = 5.8, 14.8 Hz, 1H), 4.37 (dd, *J* = 5.2, 14.8 Hz, 1H), 5.11 (s, 2H), 6.57 (bt, *J* = 5.8 Hz, 1H), 6.66 (bs, 1H), 6.88 (bt, *J* = 5.9 Hz, 1H), 7.18 (d, *J* = 8.4 Hz, 2H), 7.29 – 7.37 (m, 7H); ¹³C NMR (100 MHz, CDCl₃) δ (ppm) 28.3, 33.9, 34.9, 38.7, 42.6, 43.1, 48.0, 66.5, 80.5, 118.8, 128.2, 128.3, 128.4, 128.6, 132.2, 135.5, 137.8, 150.7, 152.7, 166.7, 169.0, 172.0; ESI-MS *m/z* 539 [M+H]⁺, 561 [M+Na]⁺.

3-(2-(1-((4-((tert-butoxycarbonyl)amino)benzyl)carbamoyl)-4-oxoazetidin-2-yl)acetamido)propanoic acid (43)

Following GP2 compound **42** (22 mg, 0.040 mmol) yielded compound **43** as a white solid (18 mg, 99%). Mp 77 – 79°C; IR (film, cm⁻¹) 3370, 1768, 1696, 1614; ¹H NMR (400 MHz, CD₃OD) δ (ppm) 1.51 (s, 9H), 2.49 (t, *J* = 6.6 Hz, 2H), 2.56 (dd, *J* = 8.4, 14.7 Hz, 1H), 2.92 (dd, *J* = 2.9, 16.1 Hz, 1H), 2.99 (dd, *J* = 4.3, 14.7 Hz, 1H), 3.23 (dd, *J* = 5.7, 16.1 Hz, 1H), 3.41 (t, *J* = 6.6 Hz, 2H), 4.27 – 4.30 (m, 1H), 4.33 – 4.39 (m, 2H), 7.21 (d, *J* = 8.5 Hz, 2H), 7.35 (d, *J* = 8.5 Hz, 2H); ¹³C NMR (100 MHz, CD₃OD) δ (ppm) 28.7, 34.8, 36.4, 39.4, 43.0, 43.8, 49.4, 81.0, 119.9, 129.0, 134.0, 139.8, 152.4, 155.3, 168.1, 171.9; ESI-MS *m/z* 449 [M+H]⁺, 471 [M+Na]⁺.

Benzyl 3-(2-(1-((4-(((tert-butoxycarbonyl)amino)methyl)phenyl)carbamoyl)-4-oxoazetidin-2-yl)acetamido)propanoate (45)

Carboxylic acid **44** (86 mg, 0.23 mmol, 1 equiv) was dissolved in a mixture of CH₂Cl₂ (2.7 mL) and CH₃CN (0.5 mL) under nitrogen. DCC (52 mg, 0.25 mmol, 1.1 equiv) was then added at 0°C. It was followed by the dropwise addition of a previously prepared solution of β-alanine benzylester *p*-toluenesulfonate salt (123 mg, 0.35 mmol, 1.5 equiv) and TEA (52 μL, 0.37 mmol, 1.6 equiv) in CH₂Cl₂ (2.9 mL). After addition of catalytic DMAP (6 mg, 0.046 mmol, 0.2 equiv), the solution was warmed to rt and left under stirring overnight. After complete consumption of the starting material (16 h) the mixture was quenched with H₂O and extracted with CH₂Cl₂ (3x10 mL). The collected organic layers were dried on Na₂SO₄ and filtered. The crude was suspended in AcOEt and the solid residual dicyclohexylurea was eliminated by filtration. The organic layer was concentrated in vacuum and purified by flash-chromatography (CH₂Cl₂/AcOEt 80:20 to 50:50) yielding compound **45** (88 mg, 71%) as a light yellow waxy solid.

IR (film, cm⁻¹) 3333, 1767, 1710, 1661, 1604; ¹H NMR (400 MHz, CDCl₃) δ (ppm) 1.44 (s, 9H), 2.54 – 2.60 (m, 3H), 3.04 (dd, *J* = 3.5, 14.8 Hz, 1H), 3.08 (dd, *J* = 3.1, 16.3 Hz, 1H), 3.28 (dd, *J* = 5.7, 16.4 Hz, 1H), 3.50 (q, *J* = 6.1 Hz, 2H), 4.21 – 4.25 (m, 2H), 4.33 – 4.38 (m, 1H), 4.89 (bt, *J* = 6.0 Hz, 1H), 5.06 (s, 2H), 6.50 (bt, *J* = 5.8 Hz, 1H), 7.20 (d, *J* = 8.3 Hz, 2H), 7.30 – 7.35 (m, 5H), 7.39 (d, *J* = 8.3 Hz, 1H), 8.48 (bs, 1H); ¹³C NMR (100 MHz, CDCl₃) δ (ppm); 28.3, 33.9, 34.9, 38.5, 42.7, 44.1, 48.4, 66.5, 79.4, 119.9, 128.2, 128.2, 128.4, 128.6, 135.0, 135.5, 136.0, 148.0, 155.8, 167.1, 168.8, 172.1; ESI-MS *m/z* 539 [M+H]⁺, 561 [M+Na]⁺.

3-(2-(1-((4-(((tert-butoxycarbonyl)amino)methyl)phenyl)carbamoyl)-4-oxoazetidin-2-yl)acetamido)propanoic acid (46)

Following GP2 compound **45** (79 mg, 0.150 mmol) yielded compound **46** as a waxy white solid (67 mg, 99%). IR (film, cm^{-1}) 3346, 1773, 1740, 1710, 1688, 1655; ^1H NMR (400 MHz, CD_3OD) δ (ppm) 1.45 (s, 9H), 2.50 (t, $J = 6.6$ Hz, 2H), 2.62 (dd, $J = 14.8, 8.2$ Hz, 1H), 3.01 (ddd, $J = 19.3, 15.5, 3.7$ Hz, 2H), 3.30 (dd, $J = 5.8$ Hz, 1H), 3.43 (t, $J = 6.7$ Hz, 2H), 4.18 (s, 2H), 4.34 – 4.43 (m, 1H), 7.23 (d, $J = 8.4$ Hz, 2H), 7.43 (d, $J = 8.4$ Hz, 2H); ^{13}C NMR (100 MHz, CD_3OD) δ (ppm) 28.8, 34.8, 36.5, 39.4, 43.1, 44.5, 49.6, 84.3, 121.1, 128.8, 136.9, 137.4, 149.7, 163.7, 168.5, 171.9, 175.6; ESI-MS m/z 561 $[\text{M}+\text{TFA}-\text{H}]^-$.

Cell culture

SK-MEL-24 cells (expressing $\alpha_v\beta_3$ integrin) were routinely grown in Eagle's Minimum Essential Medium (EMEM, Cambrex, Walkersville, MD, USA) supplemented with 10% foetal bovine serum (FBS; Life technologies, Carlsbad, CA, USA), non-essential aminoacids and sodium pyruvate. K562 cells (expressing $\alpha_5\beta_1$ integrin), Jurkat E6.1 human T cells (expressing $\alpha_4\beta_1$ and $\alpha_L\beta_2$ integrins), HEL cells (expressing $\alpha_{IIb}\beta_3$ integrin), MCF7 cells (expressing $\alpha_v\beta_5$ integrin) and HT-29 cells (expressing $\alpha_v\beta_6$ integrin) were cultured in RPMI-1640 (Life technologies) and glutamine with 10% FBS. HEL cells were a kind gift of Dr. Cecilia Prata and Laura Zambonin, while MCF7 and HT-29 cells were a kind gift of Prof. Natalia Calonghi. HEK293 cells were grown in EMEM supplemented with 10% FBS, non-essential aminoacids and L-glutamine. Cells were kept at 37°C under 5% CO_2 humidified atmosphere; 40 h prior to experiments, K562 cells were treated with 25 ng/mL PMA (Phorbol 12-myristate 13-acetate, Sigma Aldrich SRL, Milan,

Italy) to induce differentiation and to increase expression of $\alpha_5\beta_1$ integrin on cell surface . All cell lines were purchased from American Type Culture Collection (ATCC, Rockville, MD, USA).

These cell models are widely used to investigate potential agonists or antagonists of integrin-mediated cell adhesion.^{14, 38-41, 49, 65, 66, 67}

Cell adhesion assays

The assays were performed as described in Ref. 14 Briefly, for adhesion assay on SK-MEL-24, K562 and HT-29 cells 96-well plates (Corning Costar, Celbio, Milan, Italy) were coated by passive adsorption with fibronectin (10 $\mu\text{g}/\text{mL}$) overnight at 4 °C, while for MCF7 or HEL cells plates were coated with fibrinogen (10 $\mu\text{g}/\text{mL}$). Cells were counted and pre-incubated with various concentrations of each compound or with the vehicle (methanol) for 30 min at room temperature to reach ligand-receptor equilibrium. Then, the cells were plated (50,000 cells/well; for HEL cells 100000 cells/well) and incubated at room temperature for 1 h in fibronectin/fibrinogen-coated plates. All the wells were then washed with 1% BSA (bovine serum albumin) in PBS (phosphate-buffered saline) to remove non-adherent cells, and 50 μL hexosaminidase [4-nitrophenyl-N-acetyl-b-d-glucosaminide dissolved at a concentration of 7.5 mM in 0.09 M citrate buffer (pH 5) 0.5% Triton X-100 in H₂O] was added. This product is a chromogenic substrate for β -N-acetylglucosaminidase, whereby it is transformed into 4-nitrophenol; absorbance was measured at 405 nm after the addition of stopping solution [50 mM glycine and 5 mM EDTA (pH 10.4)], and the plates were read in a Victor² Multilabel Counter (PerkinElmer, Waltham, MA, USA). Reference compounds **50** (BIO-1211), Ac-Asp-Arg-Leu-Asp-Ser-OH (**48**) and cyclo(Arg-Gly-Asp-D-Phe-Val) (**49**) were purchased from Bachem

(Bubendorf, Switzerland), while H-Gly-Arg-Gly-Asp-Thr-Pro-OH (**47**) was from Sigma. Under these conditions, no significant cell adhesion was observed for bovine serum albumin (BSA)-coated plates (negative control) or nonspecific ligand-coated plates (data not shown).

For adhesion assays on Jurkat E6.1 cells, black 96-well plates were coated overnight at 4 °C with VCAM-1 or ICAM-1 (both 5 µg/mL) to study respectively adhesion mediated by $\alpha_4\beta_1$ and $\alpha_1\beta_2$ integrins. Jurkat E6.1 cells were counted and stained with CellTracker green CMFDA (12.5 µM, 30 min at 37 °C, Life Technologies). After three washes, Jurkat E6.1 cells were pre-incubated with various concentrations of each compound or with the vehicle (methanol) for 30 min at 37°C. Cells were plated (500,000/well) on coated wells and incubated for 30 min at 37 °C. After three washes, adhered cells were lysed with 0.5% Triton X-100 in PBS (30 min at 4 °C) and fluorescence was measured (Ex485 nm/Em535 nm).

Experiments were carried out in quadruplicate and repeated at least three times. Data analysis and EC₅₀ or IC₅₀ values were calculated using GraphPad Prism 5.0 (GraphPad Software, San Diego, CA, USA).

In another set of experiment, Jurkat E6.1 (500,000 cells/well) or K562 cells (50,000 cells/well) were plated in 96-wells plate previously coated directly with the most effective agonists under examination, dissolved in methanol to the final concentration of 10 µg/mL. When required, neutralizing antibodies α_5 (Chemicon International, Millipore) or α_4 (Santa Cruz Biotechnology) integrin subunit (both 10 µg/mL) or a selective $\alpha_{IIb}\beta_3$ integrin antagonist Tirofiban (**51**)¹⁴ (5-10 µM) (Sigma Aldrich) were added to the cells 10 min before plating cells on wells coated with β -lactam agonists. The number of adherent cells was determined as above described.

Competitive solid-phase binding assay on isolated integrins

To determine integrin-ligand interactions, a solid-phase binding assay was performed using purified soluble integrins and coated extracellular matrix proteins, as previously described with the following modifications.¹⁸ Flat, black 96-well plates were coated by passive adsorption with extracellular matrix ligands in carbonate buffer (15 mM Na₂CO₃, 35 mM NaHCO₃, pH 9.6) overnight at 4 °C as follow: fibronectin 0.5 µg/mL for α_vβ₃, α_vβ₆ and α₅β₁, fibrinogen 10 µg/mL for α_{IIb}β₃ and α_vβ₅, ICAM-1 for α_Lβ₂. After three washes with PBST buffer (137 mM NaCl, 2.7 mM KCl, 10 mM Na₂PO₄, 2mM KH₂PO₄, 0.01% Tween 20, pH 7.4), wells were blocked with TSB buffer (20 mM Tris-HCl, 150 mM NaCl, 1 mM CaCl₂, 1 mM MgCl₂, 1 mM MnCl₂, pH 7.5, 1% BSA) for 1 hour at room temperature. Integrins were purified as described in Supporting Information. Purified integrins were incubated with β-lactam compounds, tested at different concentrations (10⁻⁴ – 10⁻¹⁰ M), in the coated wells for one hour at room temperature. Preliminary assays ascertained the optimal concentration of each integrin binding to respective ECM (3 µg/mL for α_vβ₃ and α_vβ₅; 5 µg/mL for α_vβ₆ and α_{IIb}β₃; 10 µg/mL for α₅β₁ and α_Lβ₂). The plate was washed three times with PBST buffer and primary antibody was added for 1 hour incubation at room temperature. Integrin antibodies were purchased from: Calbiochem for α_v integrin (1:200 dilution), BD Bioscience for α_{IIb}β₃ and α₅β₁ integrins (1:200 and 1:100 dilution, respectively), Chemicon International for α_Lβ₂ (1:100 dilution). Then, secondary antibody AlexaFluor488 conjugated (1:400 dilution, ThermoFisher Scientific) was added after three washes with PBST buffer and incubated 1 hour at room temperature. After washing three times, fluorescence was measured (Ex485 nm/Em535 nm) in a Victor² Multilabel Counter.

Experiments were carried out in duplicate and repeated at least three times. Data analysis and IC₅₀ values were calculated using GraphPad Prism 5.0 (GraphPad Software, San Diego, CA, USA).

Scintillation proximity-binding assay (SPA)⁴⁹

To detect competitive binding of drugs to soluble ¹²⁵I-human FN (M_w approximately 440 kDa) bound to an antibody-captured integrin complex we employed a SPA assay, as previously described.⁴⁹ Briefly, experiments were carried out in scintillation vials; in each vial 1mg/50 ml antirabbit-coated beads (GE Healthcare Life Sciences), 200 mg of rabbit anti- α_4 integrin antibody (SantaCruz Biotechnology) and approximately 100 mg of purified $\alpha_4\beta_1$ integrin were added. The $\alpha_4\beta_1$ integrin was extracted and purified from HEK293 cells stably expressing the α_4 integrin subunit (these cells endogenously express the β_1 integrin subunit: data not shown). The cells were collected with a cell scraper; then membrane proteins were extracted and $\alpha_4\beta_1$ integrin was purified by affinity chromatography, as described.⁶⁸ The binding buffer contained Tris–HCl 25 mM pH 7,5; CaCl₂ 1 mM; MgCl₂ 1 mM; MnCl₂ 1mM; BSA 2% (w/v); phenylmethanesulfonyl fluoride (PMSF) 1 mM; aprotinin 1 mg/ml; leupeptin 50 mM. First, we allowed for the slow interaction between the α_4 integrin protein and the rabbit anti-human α_4 integrin antibody by incubating them together for 1 h at 4 °C. Then the antirabbit antibody binding beads were added, and the solution containing the three components was incubated for 2 h at 4 °C in the dark. From this point on, all incubations were conducted at room temperature. [¹²⁵I]-FN was added to the vials, which were then incubated overnight on a shaker in the dark. Nonspecific binding was determined in the presence of the specific $\alpha_4\beta_1$ integrin antagonist **50**

(BIO-1211) (100 mM). The samples were read using a LS 6500 multipurpose scintillation counter (Beckham Coulter, Fullerton, CA, USA). Experiments were carried out in triplicate and repeated at least three times. Data analysis and IC₅₀ values were calculated using GraphPad Prism 5.0 (GraphPad Software, San Diego, CA, USA).

Flow cytometry analysis.⁶⁹

Jurkat E6.1 cells were suspended in 1% BSA/HBSS (Hanks' Balanced Salt Solution, LifeTechnologies) at the concentration of 10⁶ cells/mL (100 µL/sample) and incubated with different concentration of the most effective compounds towards α₄β₁ integrin, for 30 min at 37°C. At the end of the incubation, Phycoerythrin (PE)-labeled HUTS-21 antibody (PE mouse anti-human CD29 antibody, BD Pharmingen) (20 µl/sample) was added and the cells were incubated for 45 min at room temperature. After two washes with 1% BSA/HBSS, cells were resuspended in PBS and analyzed in a Guava EasyCyte (Millipore) flow cytometry and 10,000 cells/sample were analyzed. Data were normalized with the relative fluorescence for nonspecific binding evaluated by exposing the cells to an isotype control mAb and set to 0.

HEK293 cells transfection

HEK293 cells (not expressing α_v nor β₃ integrin) were plated in 10mm dishes and at 50–60% confluence were transiently transfected with α_v⁷⁰ and β₃ plasmids using Lipofectamine2000 transfection reagent (LifeTechnologies). After 48 h from transfection, HEK293+α_vβ₃ cells were assessed to verify integrins expression: cells were incubated with a saturating concentration of

anti-human α_v or anti-human β_3 antibody for 30 min at 4 °C; subsequently, a fluorescein isothiocyanate (FITC)-conjugated secondary antibody was added for 45 min at 4 °C in the dark. After each incubation step, the cells were washed with 1% BSA/HBSS. Finally, the cells were resuspended in PBS and analyzed in a Guava EasyCyte (Millipore) flow cytometry and 10,000 cells/sample were analyzed (data not shown). α_v Integrin plasmid was a kind gift from Michael Davidson (Addgene plasmid #57345) while β_3 integrin was a kind gift of Prof. S.J. Shattil.

Western blot analysis

Western blot analysis was performed as previously described,³⁹ with the following modifications. K562 or Jurkat E6.1 cells were incubated in RPMI-1640 with 1% FBS for 16 h, while HEK293+ $\alpha_v\beta_3$ cells were serum starved in EMEM for 18 h. Plates were coated with fibronectin (10 μ g/mL) and blocked with 1% BSA. Subsequently, 4×10^6 cells were pre-incubated with different concentrations of the most effective compounds for 60 min and then were allowed to adhere for 1h on fibronectin. Cells treated with agonists were not incubated with fibronectin. Thereafter, the cells were lysed in mammalian protein extraction reagent (M-PER; Pierce, Rockford, IL, USA) supplemented with Phosphatase Inhibitor Cocktail (Sigma Aldrich SRL) for 10 min at 4°C by gentle shaking. Cell debris was removed by centrifugation (14 000 g for 15 min at 4 °C), and protein concentration was determined by BCA assay (Pierce, Rockford, IL, USA). Protein extracts were denatured at 95 °C for 3 min before loading and separation by 12% SDS-PAGE. The membranes were blocked in 5% BSA for 1 h and incubated with anti-phospho-ERK 1/2 (extracellular signal-regulated kinase 1/2) (1:1000) (Cell Signaling Technology, Danvers, MA, USA) or anti-total ERK1/2 antibodies (1:1000) (Cell Signaling Technology) overnight at

4°C. Next, the membranes were incubated with peroxidase-conjugated secondary antibodies at a 1:8,000 dilution (Santa Cruz Biotechnology). Digital images were acquired and analyzed according to a previously reported method.⁷¹

Apoptosis detection

Phycoerythrin-conjugated annexin V (annexin V-PE) and 7-amino-actinomycin D (7-AAD; Guava Nexin Reagent, Millipore) were used to determine the percentage of viable, early-apoptotic and late apoptotic/necrotic cells by flow cytometry. After three hour incubation, cells were collected and resuspended in 100 µl of complete medium. The cells were then stained with 100 µl of Nexin reagent for 20 min at room temperature in the dark, following manufacturer's instructions, and analyzed on a Guava easyCyte 5 flow cytometer (Millipore). Three populations of cells can be distinguished by this assay: viable cells (annexin V-PE and 7-AAD negative), early apoptotic cells (annexin V-PE positive and 7-AAD negative), and late stages apoptosis or necrotic cells (annexin V-PE and 7-AAD positive).

Molecular Docking

Docking calculations were run using the Schrödinger suite of programs (<http://www.schrodinger.com>) through the Maestro graphical interface.

Ligand preparation. Ionized carboxylate and neutral aniline are suggested by the Epik version 2.2⁷² as the relevant protonation states at pH = 7 for the acid and basic pharmacophoric groups of compounds **15** and **5** according to predicted pKa values of 4.1 (mono-substituted ethanoic acid and 4-oxo-butanoic acid, respectively) and 4.5 (phenyl anilinium derivative). Ionized carboxylate and protonated benzylic amine are suggested by the Epik module as the relevant protonation states at pH = 7 for ligand **1** according to predicted pKa values of 4.1 (mono-substituted ethanoic

acid) and 8.5 (benzylaminium derivative). These protonation states were considered for docking studies of the compounds.

Protein Setup. The crystal structure of the extracellular domain of the $\alpha_v\beta_3$ integrin in complex with Cilengitide and in the presence of the proadhesive ion Mn^{2+} (PDB entry 1L5G)⁶² was used for docking studies. Docking was performed only on the globular head of the integrin because the headgroup of integrin has been identified in the X-ray structure as the ligand-binding region. The protein structure was set up for docking as follows; the protein was truncated to residues 41-342 for chain α and residues 114-347 for chain β . Due to a lack of parameters in Glide version 4.5, the Mn^{2+} ions in the experimental protein structure were modeled via replacement with Ca^{2+} ions. The resulting structure was prepared using the Protein Preparation Wizard of the graphical user interface Maestro and the OPLSAA force field.

Docking. The automated docking calculations were performed using Glide (Grid-based Ligand Docking with Energetics)⁶¹ within the framework of Impact version 4.5 in a standard precision mode (SP). The grid generation step started from the extracellular fragment of the X-ray structure of the $\alpha_v\beta_3$ complex with Cilengitide, prepared as described in Protein Setup. The center of the grid-enclosing box was defined by the center of the bound ligand. The enclosing box dimensions, which are automatically deduced from the ligand size, fit the entire active site. For the docking step, the size of the bounding box for placing the ligand center was set to 12 Å. No further modifications were applied to the default settings. The Glide-Score function was used to select 10 poses for each ligand. Glide was initially tested for its ability to reproduce the crystallized binding geometry of Cilengitide. The program was successful in reproducing the experimentally found binding mode of this compound, as it corresponds to the best-scored pose (docking vs X-ray peptide backbone rmsd = 0.4 Å). To confirm our results, we built a new

docking model for the $\alpha\text{v}\beta\text{3}$ integrin using the 2016 software version (Glide version 7.0) that contains parameters for Mn^{2+} ions. The results provided by the new model are very similar to those obtained with the former model (as shown for example by the superimposition between the two models for compound (*R*)-**1** included in the Supporting Information as Figure S7).

ASSOCIATED CONTENT

Supporting Information contains Pharmacology (Figure S1 and S2), Integrin extraction and purification); Stability data at pH 7.4 and in serum for compounds **2** and **4**. Docking models of compound (*R*)-**1** using Glide v4.5 (integrin and MIDAS Ca^{2+} ion) and Glide v7.0 (integrin and MIDAS Mn^{2+} ; ^1H and ^{13}C NMR spectra of compounds **4, 5, 6, 7, 8, 9, 10, 11, 12, 14, 16, 17, 18, 19, 20, 21, 24, 25, 26, 27, 28, 29, 30, 31, 32, 33, 36, 37, 38, 39, 40, 41, 42, 43, 45, and 46**.

AUTHOR INFORMATION

Corresponding Authors

Prof. Daria Giacomini tel +39 051 209 9528 e-mail: daria.giacomini@unibo.it

Prof. Santi Mario Spampinato tel +39 051 209 1851 e-mail: santi.spampinato@unibo.it

Author Contributions

The manuscript was written through contributions of all authors. All authors have given approval to the final version of the manuscript.

Funding Sources

All authors received funds from the project MIUR PRIN project 2010NRREPL: Synthesis and biomedical applications of tumor-targeting peptidomimetics. D.G., P.G., and S.P. also received funds from University of Bologna (RFO funding).

ACKNOWLEDGMENT

DG would like to thank L. Turrini, M. Moncelli, M. Nagakawa, S. Carpinelli, L. Merlo for technical assistance.

ABBREVIATION USED

RGD, arginyl-glycyl-aspartic acid tripeptide; NaHMDSA, sodium hexamethyldisilylamide; TEA, triethylamine; PTSA, pyridiniumparatoluensulfonic acid; EDC, N-(3-dimethylaminopropyl)-N'-ethylcarbodiimide hydrochloride; DCC, dicyclohexylcarbodiimide; VCAM-1, vascular cell adhesion protein 1; ICAM, intercellular adhesion molecule 1; SD, standard deviation; c(-RGDfV), cyclo(-Arg-Gly-Asp-D-Phe-Val); fibronectin, FN;

REFERENCES

- 1 For recent reviews see: Arya, N; Jagdale, A. Y.; Patil, T. A.; Yeramwar, S. S.; Holikatti, S. S.; Dwivedi, J.; Shishoo, C. J.; Jain, K. S. The chemistry and biological potential of azetidin-2-ones. *Eur. J. Med. Chem.* **2014**, *74*, 619-656.
- 2 Galletti, P.; Giacomini, D. Monocyclic β -Lactams: New structures for new biological activities. *Curr. Med. Chem.* **2011**, *18*, 4265-4283.

- 3 Mehta, P. D.; Sengar, N. P. S.; Pathak, A. K. 2-Azetidinone -a new profile of various pharmacological activities. *Eur. J. Med. Chem.* **2010**, *45*, 5541-5560.
- 4 Crauste, C.; Froeyen, M.; Anné, J.; Herdewijn P. Asymmetric synthesis of new β -lactam lipopeptides as bacterial signal peptidase I antagonists. *Eur. J. Org. Chem.* **2011**, 3437-3449.
- 5 Dražić, T.; Sachdev, V.; Leopold, C.; Patankar, J.V.; Malnar, M.; Hećimović, S.; Levak-Frank, S.; Habuš, I.; Kratky, D. Synthesis and evaluation of novel amide amino- β -lactam derivatives as cholesterol absorption antagonists. *Bioorg. Med. Chem.* **2015**, *23*, 2353-2359.
- 6 Feledziak, M.; Michaux, C.; Lambert, D.M.; Marchand-Brynaert, J. An unprecedented reversible mode of action of β -lactams for the inhibition of human fatty acid amide hydrolase (hFAAH). *Eur. J. Med. Chem.* **2013**, *60*, 101-111.
- 7 O'Boyle, N. M.; Knox, A. J. S.; Price, T. T.; Williams D. C.; Zisterer, D. M.; Lloyd, D.G.; Meegan, M. J. Lead identification of β -lactam and related imine antagonists of the molecular chaperone heat shock protein 90. *Bioorg. Med. Chem.* **2011**, *19*, 6055-6068.
- 8 Galletti, P.; Quintavalla, A.; Ventrici, C.; Giannini, G.; Cabri, W.; Penco, S.; Gallo, G.; Vincenti, S.; Giacomini, D. Azetidinones as zinc-binding groups to design selective HDAC8 antagonists. *ChemMedChem*, **2009**, *4*, 1991-2001.

- 9 Wong, P. C.; Crain, E. J.; Watson, C.A.; Schumacher, W.A. A small-molecule factor XIa antagonist produces antithrombotic efficacy with minimal bleeding time prolongation in rabbits. *J. Thromb. Thrombolysis* **2011**, *32*, 129-137.
- 10 Alcaide, B; Almendros, P; Aragoncillo, C. Highly reactive 4-membered ring nitrogen-containing heterocycles: synthesis and properties. *Curr. Opin. Drug Di. De.* **2010**, *13*, 685-697.
- 11 Aizpurua, J. M.; Ganboa, J. I.; Palomo, C.; Loinaz, I.; Oyarbide, J.; Fernandez, X.; Balentova, E.; Fratila, R. M.; Jimenez, A.; Miranda, J. I.; Laso, A.; Avila, S.; Castrillo, J. L. Cyclic RGD beta-lactam peptidomimetics induce differential gene expression in human endothelial cells. *ChemBioChem* **2011**, *12*, 401-405.
- 12 Aizpurua, J. M.; Oyarbide, J.; Fernandez, X.; Miranda, J. I.; Ganboa, J. I.; Avila, S.; Castrillo, J. L. Preparation of pro-angiogenic beta-lactams cyclotetrapeptides. Eur. Pat. Appl. 2012, EP 2407478 A1 20120118.
- 13 Aizpurua, J. M.; Ganboa, J. I.; Palomo, C.; Loinaz, I.; Miranda, J. I. Beta-Lactams RGD cyclopeptides containing gamma turns. PCT Int. Appl. 2006, WO 2006048473 A1 20060511.
- 14 Galletti, P.; Soldati, R.; Pori, M.; Durso, M.; Tolomelli, A.; Gentilucci, L.; Deianira Dattoli, S.; Baiula, M.; Santi Spampinato, M.; Giacomini, D. Targeting integrins $\alpha_v\beta_3$ and $\alpha_5\beta_1$ with new β -lactam derivatives. *Eur. J. Med. Chem.* **2014**, *83*, 284-293.
- 15 Plow, E.F.; Haas, T.A.; Zhang, L.; Loftus, J.; Smith, J.W. Ligand binding to integrins. *J. Biol. Chem.* **2000**, *275*, 21785-21788.

- 16 Busk, M.; Pytela, R.; Sheppard, D. Characterization of the integrin $\alpha_v\beta_6$ as a fibronectin-binding protein. *J. Biol. Chem.* **1992**, *267*, 5790–5796.
- 17 Aumailley, M.; Gurrath, M.; Müller, G.; Calvete, J.; Timpl, R.; Kessler, H. Arg-Gly-Asp constrained within cyclic pentapeptides. Strong and selective inhibitors of cell adhesion to vitronectin and laminin fragment P1. *FEBS Lett.* **1991**, *291*, 50–54.
- 18 Frank, A. O.; Otto, E.; Mas-Moruno, C.; Schiller, H. B.; Marinelli, L.; Cosconati, S.; Bochen, A.; Vossmeier, D.; Zahn, G.; Stragies, R.; Novellino, E.; Kessler, H. Conformational control of integrin-subtype selectivity in isoDGR peptide motifs: a biological switch. *Angew. Chem. Int. Ed. Engl.* **2010**, *49*, 9278-9281.
- 19 Neubauer, S.; Rechenmacher, F.; Brimiouille, R.; Di Leva, F. S.; Bochen, A.; Sobahi, T. R.; Schottelius, M.; Novellino, E.; Mas-Moruno, C.; Marinelli, L.; Kessler, H. Pharmacophoric modifications lead to superpotent $\alpha_v\beta_3$ integrin ligands with suppressed $\alpha_5\beta_1$ activity. *J. Med. Chem.* **2014**, *57*, 3410-3417.
- 20 Bochen, A.; Marelli, U. K.; Otto, E.; Pallarola, D.; Mas-Moruno, C.; Di Leva, F. S.; Boehm, H.; Spatz, J. P.; Novellino, E.; Kessler, H.; Marinelli, L. Biselectivity of isoDGR peptides for fibronectin binding integrin subtypes $\alpha_5\beta_1$ and $\alpha_v\beta_6$: conformational control through flanking amino acids. *J. Med. Chem.* **2013**, *56*, 1509-1519.
- 21 Maltsev, O. V.; Marelli, U. K.; Kapp, T. G.; Di Leva, F. S.; Di Maro, S.; Nieberler, M.; Reuning, U.; Schwaiger, M.; Novellino, E.; Marinelli, L.; Kessler, H. Stable peptides

- instead of stapled peptides: highly potent $\alpha_v\beta_6$ -selective integrin ligands. *Angew. Chem. Int. Ed. Engl.* **2016** *55*, 1535-1539.
- 22 Campbell, I. D.; Humphries, M. J. Molecular mechanism of inside-out integrin regulation *Cold Spring Harb. Perspect. Biol.* **2011**, *3*:a004994, doi : 10.1101/cshperspect.a004994.
- 23 Luo, B-H.; Carman, C. V.; Springer, T. A. Structural basis of integrin regulation and signaling. *Ann. Rev. Immunol.* **2007**, *25*, 619-647.
- 24 Hynes, R. O. Integrins: bidirectional, allosteric signaling machines. *Cell* **2002**, *110*, 673-687.
- 25 Barczyk, M.; Carracedo, S.; Gullberg, D. Integrins. *Cell Tissue Res.* **2010**, *339*, 269-280.
- 26 Kim, S-H.; Turnbull, J.; Guimond, S. Extracellular matrix and cell signalling: the dynamic cooperation of integrin, proteoglycan and growth factor receptor. *J. Endocrinol.* **2011**, *209*, 139-151.
- 27 Sheldrake, H. M.; Patterson, L. H. Strategies to inhibit tumor associated integrin receptors: rationale for dual and multi-antagonists. *J. Med. Chem.* **2014**, *57*, 6301-6315.
- 28 Dong, X.; Hudson, N. E.; Lu, C.; Springer, T. A. Structural determinants of integrin β -subunit specificity for latent TGF- β . *Nat. Struct. Mol. Biol.* **2014**, 1091-1096.
- 29 Yee K. L.; Weaver V. M.; Hammer D. A. Integrin-mediated signalling through the MAP-kinase pathway. *IET Syst. Biol.* **2008**, *2*, 8-15.

- 30 Marelli, U. K.; Rechenmacher, F.; Sobahi, T. R.; Mas-Moruno, C.; Kessler, H. Tumor targeting via integrin ligands. *Front. Oncol.* **2013**, *3*, 1-12, and references cited therein.
- 31 Celik, E.; Faridi, M. H.; Kumar, V.; Deep, S.; Moy, V. T.; Gupta, V. Agonist leukadherin-1 increases CD11b/CD18-dependent adhesion via membrane tethers. *Biophys. J.* **2013**, *105*, 2517-2727.
- 32 Khan, S. Q.; Guo, L.; Cimbaluk, D. J.; Elshabrawy, H.; Faridi, M. H.; Jolly, M.; George, J. F.; Agarwal, A.; Gupta, V. A. Small molecule β_2 integrin agonist improves chronic kidney allograft survival by reducing leukocyte recruitment and accompanying vasculopathy. *Front. Med.* **2014**, *1*, 1-11
- 33 Yang, W.; Carman, C.V.; Kim, M.; Salas, A.; Shimaoka, M.; Springer, T.A. A small molecule agonist of an integrin, $\alpha_1\beta_2$. *J. Biol. Chem.* **2006**, *281*, 37904-37912.
- 34 Vanderslice, P.; Biediger, R. J.; Woodside, D. G.; Brown, W. S.; Khounlo, S.; Warier, N. D.; Gundlach, C.W.^{4th}; Caivano, A. R.; Bornmann, W. G.; Maxwell, D. S.; McIntyre, B.W.; Willerson, J. T.; Dixon, R.A. Small molecule agonist of very late antigen-4 (VLA-4) integrin induces progenitor cell adhesion. *J. Biol. Chem.* **2013**, *288*, 19414-19428.
- 35 Du, X. P.; Plow, E. F.; Frelinger, A. L. 3rd; O'Toole, T. E.; Loftus, J. C.; Ginsberg, M. H. Ligands "activate" integrin $\alpha_{IIb}\beta_3$ (platelet GPIIb-IIIa). *Cell* **1991**, *65*, 409-416
- 36 Cabrele, C.; Martinek, T. A.; Reiser, O.; Berlicki, Ł. Peptides containing β -amino acid patterns: challenges and successes in medicinal chemistry. *J. Med. Chem.* **2014**, *57*, 9718-9739.

- 37 Springer, T. A.; Wang, J.-H. The three-dimensional structure of integrins and their ligands, and conformational regulation of cell adhesion. *Adv. Protein Chem.* **2004**, *68*, 29-63.
- 38 Tolomelli, A.; Gentilucci, L. Mosconi, E.; Viola, A.; Dattoli, S. D.; Baiula, M.; Spampinato, S. M.; Belvisi, L.; Civera, M. Development of isoxazoline-containing peptidomimetics as dual $\alpha_v\beta_3$ and $\alpha_5\beta_1$ integrin ligands. *ChemMedChem* **2011**, *6*, 2264-2272.
- 39 Tolomelli, A.; Baiula, M.; Belvisi, L.; Viola, A.; Gentilucci, L.; Troisi, S.; Dattoli, S. D.; Spampinato, S. M.; Civera, M.; Juaristi, E. Modulation of $\alpha_v\beta_3$ and $\alpha_5\beta_1$ integrin-mediated adhesion by dehydro- β -amino acids containing peptidomimetics. *Eur. J. Med. Chem.* **2013**, *66*, 258-268.
- 40 Benfatti, F.; Cardillo, G.; Fabbroni, S.; Galzerano, P.; Gentilucci, L.; Juris, R.; Tolomelli, A.; Baiula, M.; Sparta, A.; Spampinato, S. Synthesis and biological evaluation of non-peptide $\alpha_v\beta_3/\alpha_5\beta_1$ integrin dual antagonists containing 5,6-dihydropyridin-2-one scaffolds. *Bioorg. Med. Chem.* **2007**, *15*, 7380-7390.
- 41 Tolomelli, A.; Baiula, M.; Viola, A.; Ferrazzano, L.; Gentilucci, L.; Dattoli, S. D.; Spampinato, S.; Juaristi, E.; Escudero, M. Dehydro- β -proline containing $\alpha_4\beta_1$ integrin antagonists: stereochemical recognition in ligand-receptor interplay. *ACS Med. Chem. Lett.* **2015**, *6*, 701-706.
- 42 Lin, K. C.; Ateeq, H. S.; Hsiung, S. H.; Chong, L. T.; Zimmermann, C. N.; Castro, A.; Lee, W. C.; Hammond, C. E.; Kalkunte, S.; Chen, L. L.; Pepinsky, R. B.; Leone, D. R.;

- Sprague, A. G.; Abraham, W. M.; Gill, A.; Lobb, R. R.; Adams, S. P. Selective, tight binding antagonists of integrin $\alpha_4\beta_1$ that inhibit allergic airway responses. *J. Med. Chem.* **1999**, *42*, 920-934.
- 43 Pitts, W. J.; Wityak, J.; Smallheer, J. M.; Tobin, A. E.; Jetter, J. W.; Buynitsky, J. S.; Harlow, P. P.; Solomon, K. A.; Corjay, M. H.; Mousa, S. A.; Wexler, R.R.; Jadhav, P. K. Isoxazolines as potent antagonists of the integrin $\alpha_v\beta_3$. *J. Med. Chem.* **2000**, *43*, 27-40.
- 44 Broccolo, F.; Cainelli, G.; Caltabiano, G.; Cocuzza, C. E. A.; Fortuna, C. G.; Galletti, P.; Giacomini, D.; Musumarra, G.; Musumeci, R.; Quintavalla, A. Design, synthesis, and biological evaluation of 4-alkyliden-beta lactams: new products with promising antibiotic activity against resistant bacteria. *J. Med. Chem.* **2006**, *49*, 2804-2811.
- 45 Cainelli, G.; Giacomini, D.; Galletti, P.; Quintavalla, A. Synthesis of novel 4-(2-oxoethylidene)azetid-2-ones by a Lewis acid mediated reaction of acyldiazo compounds. *Eur. J. Org. Chem.* **2003**, 1765-1774
- 46 Ito, Y.; Terashima, S. A highly stereoselective synthesis of a key intermediate of 1-beta-methylcarbapenems employing the Reformatsky reaction of 3-(2-bromopropionyl)-2-oxazolidone derivatives. *Tetrahedron Lett.* **1987**, *28*, 6625-6628.
- 47 Gurrath, M.; Müller, G.; Kessler, H.; Aumailley, M.; Timpl, R. Conformation/activity studies of rationally designed potent anti-adhesive RGD peptides. *Eur. J. Biochem.* **1992** *210*, 911-921.

- 48 Mas-Moruno, C.; Rechenmacher, F.; Kessler, H. Cilengitide: the first anti-angiogenic small molecule drug candidate design, synthesis and clinical evaluation. *Anticancer Agents Med. Chem.* **2010**, 753-68.
- 49 Qasem, A. R.; Bucolo, C.; Baiula, M.; Spartà, A.; Govoni, P.; Bedini, A.; Fasci, D.; Spampinato, S. Contribution of $\alpha_4\beta_1$ integrin to the antiallergic effect of levocabastine. *Biochem. Pharmacol.* **2008**, 76, 751-762.
- 50 Bednar, R. A.; Gaul, S. L.; Hamill, T. G.; Egbertson, M. S.; Shafer, J. A.; Hartman, G. D.; Gould, R. J.; Bednar, B. Identification of low molecular weight GP IIb/IIIa antagonists that bind preferentially to activated platelets. *J Pharmacol. Exp. Ther.* **1998**, 285, 1317-1326.
- 51 Adams, J.; Anderson, E. C.; Blackham, E. E.; Chiu, Y. W.; Clarke, T.; Eccles, N.; Gill, L. A.; Haye, J. J.; Haywood, H. T.; Hoenig, C. R.; Kausas, M.; Le, J.; Russell, H. L.; Smedley, C.; Tipping, W.; J.; Tongue, T.; Wood, C. C.; Yeung, J.; Rowedder, J. E.; Fray, M. J.; McNally, T.; Macdonald, S. J. Structure activity relationships of α_v integrin antagonists for pulmonary fibrosis by variation in aryl substituents. *ACS Med. Chem. Lett.* **2014**, 5, 1207-1212.
- 52 Wandzik, K.; Zahn, C.; Dassler, K.; Fuchs, H. Substantial changes of cellular iron homeostasis during megakaryocytic differentiation of K562 cells. *Develop. Growth Differ.* **2009**, 51, 555-565.

- 53 Cox, B. D.; Natarajan, M.; Stettner, M. R.; Gladson, C. L. New concepts regarding focal adhesion kinase promotion of cell migration and proliferation. *J. Cell Biochem.* **2006**, *99*, 35-52.
- 54 Conner, S. R.; Scott, G.; Aplin, A. E. Adhesion-dependent activation of the ERK1/2 cascade is by-passed in melanoma cells. *J. Biol. Chem.* **2003**, *278*, 34548-34554.
- 55 Luo, B. H.; Springer, T. A. Integrin structures and conformational signaling. *Curr. Opin. Cell Biol.* **2006**, *18*, 579-586.
- 56 Margadant, C.; Monsuur, H. N.; Norman, J. C.; Sonnenberg, A. Mechanisms of integrin activation and trafficking. *Curr. Opin. Cell. Biol.* **2011**, *23*, 607-614.
- 57 Johansson, M. W.; Mosher, D. F. Integrin activation states and eosinophil recruitment in asthma. *Front Pharmacol.* **2013**, *4*, n°33, 1-9.
- 58 Luque, A.; Gomez, M.; Puzon, W.; Takada, Y.; Sanchez-Madrid, F.; Cabanas, C. J. Activated conformations of very late activation integrins detected by a group of antibodies (HUTS) specific for a novel regulatory region (355-425) of the common beta 1 chain. *J. Biol. Chem.* **1996**, *271*, 11067-11075.
- 59 Manzoni, L.; Belvisi, L.; Arosio, D.; Civera, M.; Pilkington-Miksa, M.; Potenza, D.; Caprini, A.; Araldi, E. M. V.; Monferini, E.; Mancino, M.; Podestà, F.; Scolastico, C. Cyclic RGD-including functionalized azabicycloalkane amino acids as potent integrin antagonists for tumor targeting. *ChemMedChem* **2009**, *4*, 615-632.

- 60 Marchini, M.; Mingozi, M.; Colombo, R.; Guzzetti, I.; Belvisi, L.; Vasile, F.; Potenza, D.; Piarulli, U.; Arosio, D.; Gennari, C. Cyclic RGD-peptidomimetics containing bifunctional diketopiperazine scaffolds as new potent integrin ligands. *Chem. Eur. J.* **2012**, *18*, 6195-6207.
- 61 Glide, version 4.5, 2007, Schrödinger, LLC, New York, NY (USA).
- 62 Xiong, J. P.; Stehle, T.; Zhang, R.; Joachimiak, A.; French, M.; Goodman, S. L.; Arnaout, M. A. Crystal structure of the extracellular segment of integrin $\alpha_V\beta_3$ in complex with an Arg-Gly-Asp ligand. *Science* **2002**, *296*, 151-155.
- 63 Van Agthoven, J. F.; Xiong, J. P.; Alonso, J. L.; Rui, X.; Adair, B. D.; Goodman, S. L.; Arnaout, M. A. Structural basis for pure antagonism of integrin $\alpha_V\beta_3$ by a high-affinity form of fibronectin. *Nat. Struct. Mol. Biol.* **2014**, *21*, 383-388.
- 64 Lee, J.; Jin, M-K.; Kang, S-U.; Kim, S. Y.; Lee, J.; Shin, M.; Hwang, J.; Cho, S.; Choi, Y-S.; Choi, H-K.; Kim, S-E.; Suh, Y-G.; Lee, Y-S.; Kim, Y-H.; Ha, H-J.; Toth, A.; Pearce, L. V.; Tran, R.; Szabo, T.; Welter, J. D.; Lundberg, D. J.; Wang, Y.; Lazar, J.; Pavlyukovets, V. A.; Morgan, M. A.; Blumberg, P. M. Analysis of structure–activity relationships for the ‘B-region’ of N-(4-t-butylbenzyl)-N’-[4-(methyl sulfonylamino)benzyl]-thiourea analogues as TRPV1 antagonists. *Bioorg. Med. Chem. Lett.*, **2005**, *15*, 4143-4150.
- 65 Boudignon-Proudhon, C.; Patel, P. M.; Parise, L. V. Phorbol ester enhances integrin $\alpha_{IIb}\beta_3$ -dependent adhesion of human erythroleukemic cells to activation-dependent monoclonal antibodies. *Blood* **1996**, *87*, 968-976.

- 66 Boys, M. L.; Schretzman, L. A.; Chandrakumar, N. S.; Tollefson, M. B.; Mohler, S. B.; Downs, V. L.; Penning, T. D.; Russell, M. A.; Wendt, J. A.; Chen, B. B.; Stenmark, H. G.; Wu, H.; Spangler, D. P.; Clare, M.; Desai, B. N.; Khanna, I. K.; Nguyen, M. N.; Duffin, T.; Engleman, V. W.; Finn, M. B.; Freeman, S. K.; Hanneke, M. L.; Keene, J. L.; Klover, J. A.; Nickols, G. A.; Nickols, M. A.; Steininger, C. N.; Westlin, M.; Westlin, W.; Yu, Y. X.; Wang, Y.; Dalton, C. R.; Norring, S. A. Convergent, parallel synthesis of a series of beta-substituted 1,2,4-oxadiazole butanoic acids as potent and selective alpha₂beta₂ receptor antagonists. *Bioorg. Med. Chem. Lett.* **2006**, *16*, 839-844.
- 67 Taherian, A.; Li, X.; Liu, Y.; Haas, T. A. Differences in integrin expression and signaling within human breast cancer cells. *BMC Cancer* **2011**, *11*, 293 (1-15).
- 68 Solorzano, C.; Bouquelet, S.; Pereyra, M. A.; Blanco-Favela, F.; Slomianny, M. C.; Chavez, R.; Lascurain, R.; Zenteno, E.; Agundis, C. Isolation and characterization of the potential receptor for wheat germ agglutinin from human neutrophils. *Glycoconj. J.* **2006**, *23*, 591-598.
- 69 Njus, B. H.; Chigaev, A.; Waller, A.; Wlodek, D.; Ostopovici-Halip, L.; Ursu, O.; Wang, W.; Oprea, T. I.; Bologa, C. G.; Sklar, L. A. Conformational mAb as a tool for integrin ligand discovery. *Assay Drug Dev Technol.* **2009**, *7*, 507-515.
- 70 McKinney, S. A.; Murphy, C. S.; Hazelwood, K. L.; Davidson, M. W.; Looger, L. L. A bright and photostable photoconvertible fluorescent protein. *Nat. Methods.* **2009**, *6*, 131-133.

- 71 Bedini, A.; Baiula, M.; Spampinato, S. Transcriptional activation of human mu-opioid receptor gene by insulin-like growth factor-I in neuronal cells is modulated by the transcription factor REST. *J. Neurochem.* **2008**, *105*, 2166-78.
- 72 Epik, version 2.2, 2011, Schrödinger, LLC, New York, NY (USA).

Table of Contents Graphics

